AD-A072 742 ARMY ELECTRONICS RESEARCH AND DEVELOPMENT COMMAND FO--ETC F/G 20/1
SHALLOW BULK ACOUSTIC WAVES.(U)
JUN 79 A BALLATO, T LUKASZEK

UNCLASSIFIED DELET-TR-79-13 NL

1 OF 1
AD
A072742

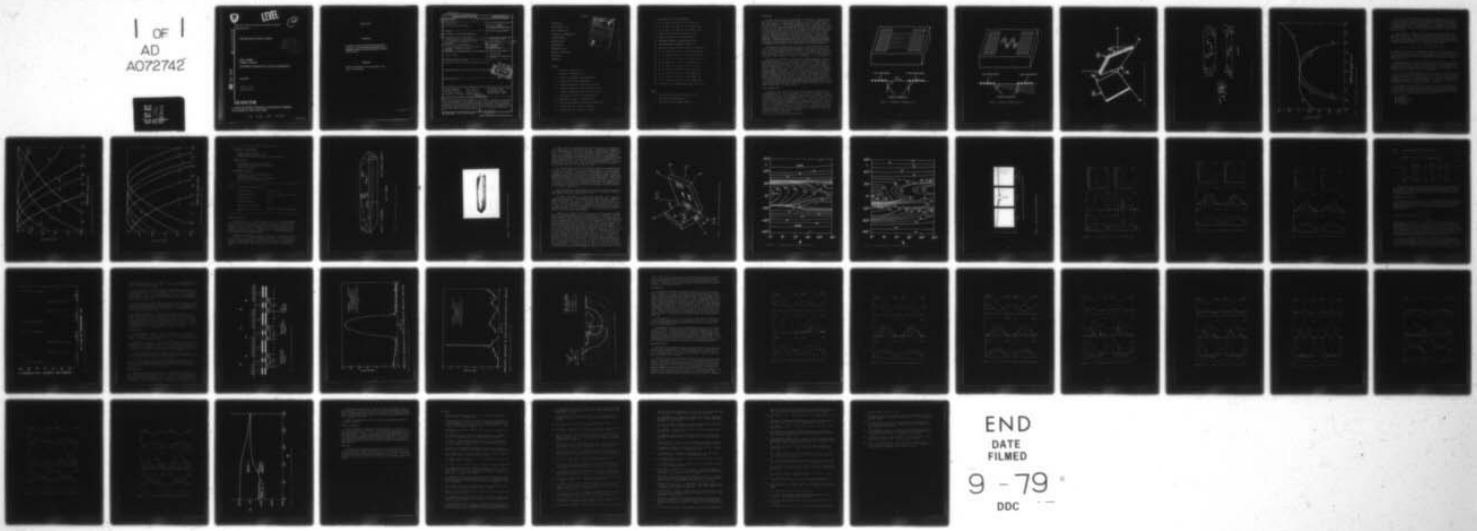

END
DATE FILMED
9-79
DDC

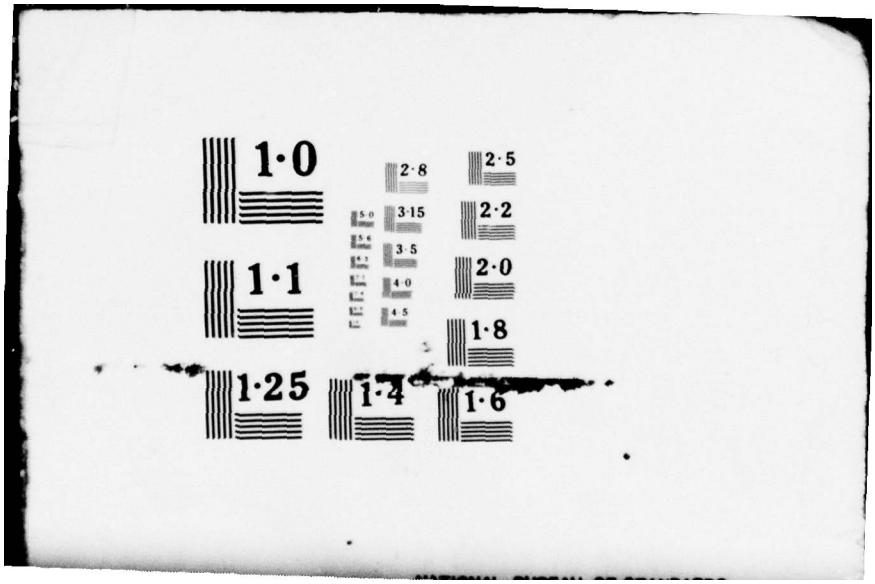
1·0
1·1
1·25
2·8
3·15
3·5
4·0
4·5
2·5
2·2
2·0
1·8
1·4
1·6

LEVEL II

(12)
B.S.

RESEARCH AND DEVELOPMENT TECHNICAL REPORT

DELET-TR-79-13



# SHALLOW BULK ACOUSTIC WAVES



Arthur Ballato
Theodore Lukaszek

ELECTRONICS TECHNOLOGY & DEVICES LABORATORY

June 1979





ERADCOM

US ARMY ELECTRONICS RESEARCH & DEVELOPMENT COMMAND
FORT MONMOUTH, NEW JERSEY 07703

# NOTICES

## Disclaimers

The citation of trade names and names of manufacturers in this report is not to be construed as official Government indorsement or approval of commercial products or services referenced herein.

## Disposition

Destroy this report when it is no longer needed. Do not return it to the originator.

UNCLASSIFIED

SECURITY CLASSIFICATION OF THIS PAGE (When Data Entered)

| REPORT DOCUMENTATION PAGE | READ INSTRUCTIONS BEFORE COMPLETING FORM |
|---|---|
| 1. REPORT NUMBER: DELET-TR-79-13 (14) | 2. GOVT ACCESSION NO. / 3. RECIPIENT'S CATALOG NUMBER |
| 4. TITLE (and Subtitle): Shallow Bulk Acoustic Waves (6) | 5. TYPE OF REPORT & PERIOD COVERED: Technical Report (9) |
| | 6. PERFORMING ORG. REPORT NUMBER |
| 7. AUTHOR(s): Arthur Ballato and Theodore Lukaszek (10) | 8. CONTRACT OR GRANT NUMBER(s) |
| 9. PERFORMING ORGANIZATION NAME AND ADDRESS: US Army Electronics Technology & Devices Laboratory, (ERADCOM) Ft. Monmouth, NJ, 07703 DELET-MM | 10. PROGRAM ELEMENT, PROJECT, TASK AREA & WORK UNIT NUMBERS: (16) ILI 62705 AH94 09 011 (17) 09 |
| 11. CONTROLLING OFFICE NAME AND ADDRESS: US Army Electronics Research & Development Command, Fort Monmouth, NJ 07703 DELET-MM | 12. REPORT DATE (11): June 1979 / 13. NUMBER OF PAGES: 44 |
| 14. MONITORING AGENCY NAME & ADDRESS (if different from Controlling Office): (12) 49 p | 15. SECURITY CLASS. (of this report): UNCLASSIFIED / 15a. DECLASSIFICATION/DOWNGRADING SCHEDULE |

16. DISTRIBUTION STATEMENT (of this Report)

Approved for public release; distribution unlimited.



17. DISTRIBUTION STATEMENT (of the abstract entered in Block 20, if different from Report)

18. SUPPLEMENTARY NOTES

19. KEY WORDS (Continue on reverse side if necessary and identify by block number)

| | | |
|---|---|---|
| Crystal resonators | AT-cut quartz | Shallow Bulk Acoustic Waves |
| Crystal oscillators | Quartz crystals | Bulk Acoustic Waves |
| Piezoelectric crystals | Frequency control | Surface Acoustic Waves |
| Piezoelectric vibrators | Frequency-Temperature Characteristics | Doubly Rotated Crystals |

20. ABSTRACT (Continue on reverse side if necessary and identify by block number)

Shallow bulk acoustic wave propagation in piezoelectric crystals is considered from the standpoint of work reported to date. It is compared to bulk and surface acoustic waves as to properties and device potential. Singly and doubly rotated cuts are considered, as are piezoelectric transduction, energy trapping, equivalent networks, as well as areas of future work such as new materials, other than quartz, and nonlinear effects.

A10698

DD FORM 1 JAN 73 1473 EDITION OF 1 NOV 65 IS OBSOLETE

UNCLASSIFIED

SECURITY CLASSIFICATION OF THIS PAGE (When Data Entered)

CONTENTS

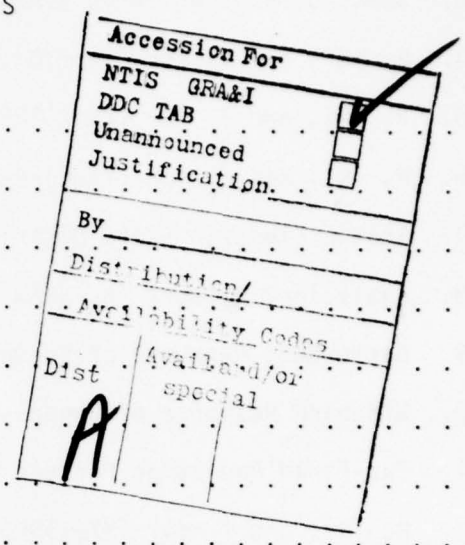




FIGURES:

TABLES:

## INTRODUCTION

The past forty years have brought about a revolution in frequency control and acoustic signal processing capabilities.[1-66]* The most recent achievements have been due in large measure to the development of surface acoustic wave (SAW) devices[1-7]. These have supplemented, and in some cases taken over various functions formerly performed by bulk acoustic wave (BAW) devices[8], particularly in the area of filtering. At the same time, SAW technology expanded to create entirely new signal processing capabilities based on the availability of the wave as a spatially distributed function at the crystal surface. Bulk wave components, meanwhile, had also found new uses. Foremost among these are new cuts that exhibit compensation of nonlinear elastic effects, leading to resonators that are ultra-stable even under severe environmental conditions. Both BAW and SAW devices profit from the favorable electromagnetic/acoustic velocity ratio which assures significant miniaturization and decreased weight with respect to the corresponding electromagnetic devices.

More recently, attention has been given to a new type of acoustic wave device, utilizing bulk waves that travel nearly parallel to the crystal surface. These are known as shallow bulk acoustic waves (SBAW), or as surface-skimming bulk waves (SSBW), and are the topic of this report. Most of the work reported to date is due to Lewis[9-18] and to Kagiwada[18-28]. Other applicable analyses are due to Mitchell[29], Wagers[30], Jhunjhunwala, et al.[31], and Lee[32].

Of particular importance to the operation of SBAW components is the interdigital transducer (IDT), consisting of interleaved electrode strips, between which the generating electric field is applied via a signal source, or the received field is detected. The IDT array was first applied to the production of BAW signals[33,34], then to SAW devices[35], and finally to SBAW devices[9]. Figures 1 and 2 show, in cross-section, the launching and reception of SAW and SBAW, respectively. Typical energy distributions are also shown; the SAW energy is confined largely within one wavelength of the surface, with evanescent behavior in the direction of the depth. The SBAW, on the other hand, is launched from the IDT array as a shallow beam of energy with real propagation wavenumbers both parallel to the surface and in the depth direction. Without further development, the SBAW device shown would be of little use if the input and output were separated by many wavelengths, because of the large energy losses encountered; fortunately these may be obviated to a large extent as described in a later section.

## SINGLY ROTATED CUTS

Crystal cuts are specified[36] by their orientations with respect to the crystallographic axes. A singly rotated cut is one that undergoes one rotation about an axis; a typical example is the rotated-Y-cut shown in Figure 3(a) and denoted as $(YX\ell)\theta$. The most popular such cut is the BAW AT-cut, seen in Figure 4 oriented within a cultured quartz bar. Its success is primarily due to the superior frequency-temperature (f-T) characteristic, which is shown in Figure 5. Also shown in this figure is the curve for the SAW ST-cut which is close in orientation to the AT. For the AT cut, $\theta = +35.25^{\circ}$, while for the ST cut, $\theta = +42.75^{\circ}$. Another BAW cut, having a zero temperature coefficient (TC) of frequency exists. This is the BT cut, at $\theta = -49.20^{\circ}$; its frequency-temperature curve is also shown in Figure 5.

* See list of references beginning on page 40.

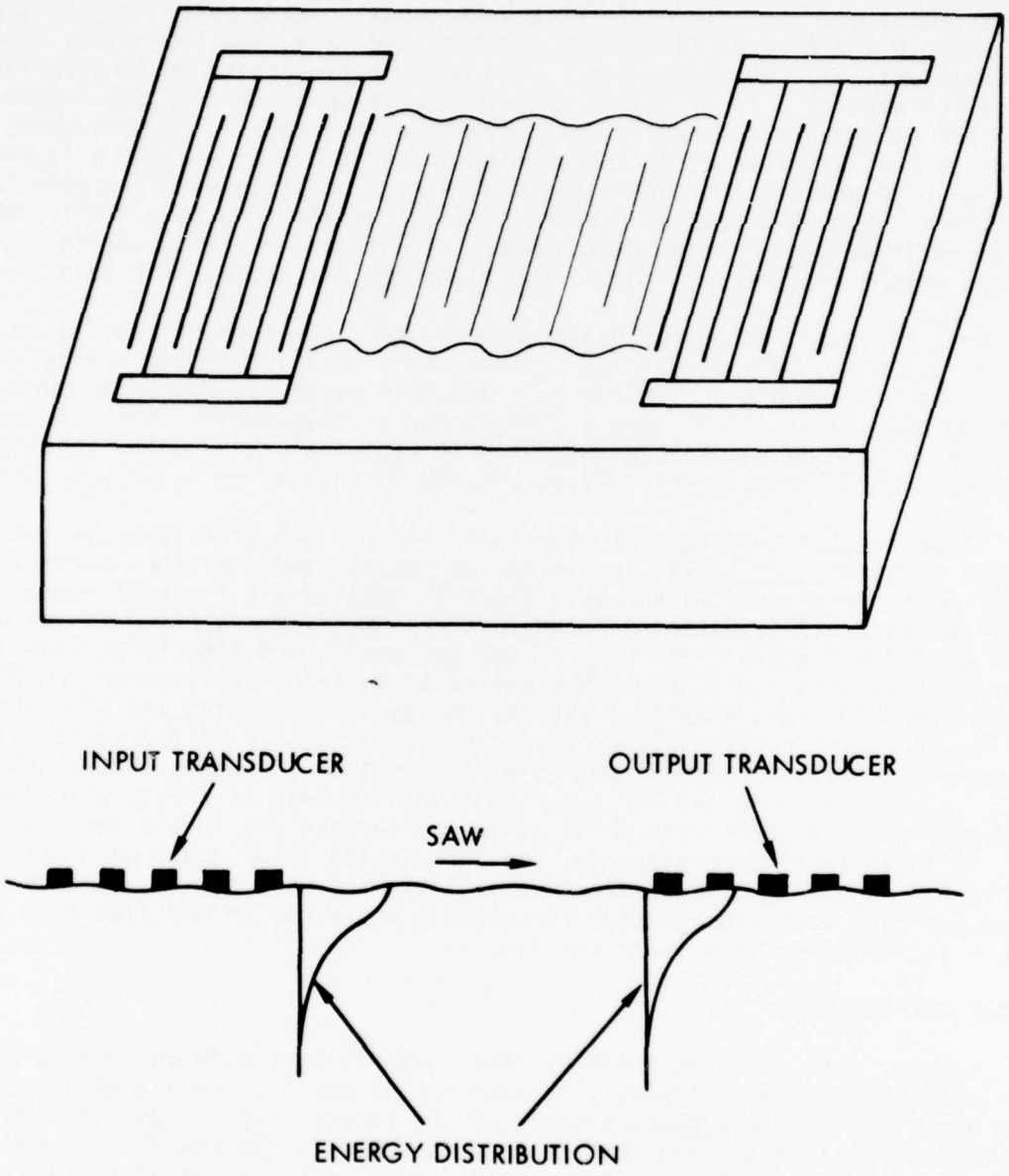


FIGURE 1. Schematic of SAW Delay Line.

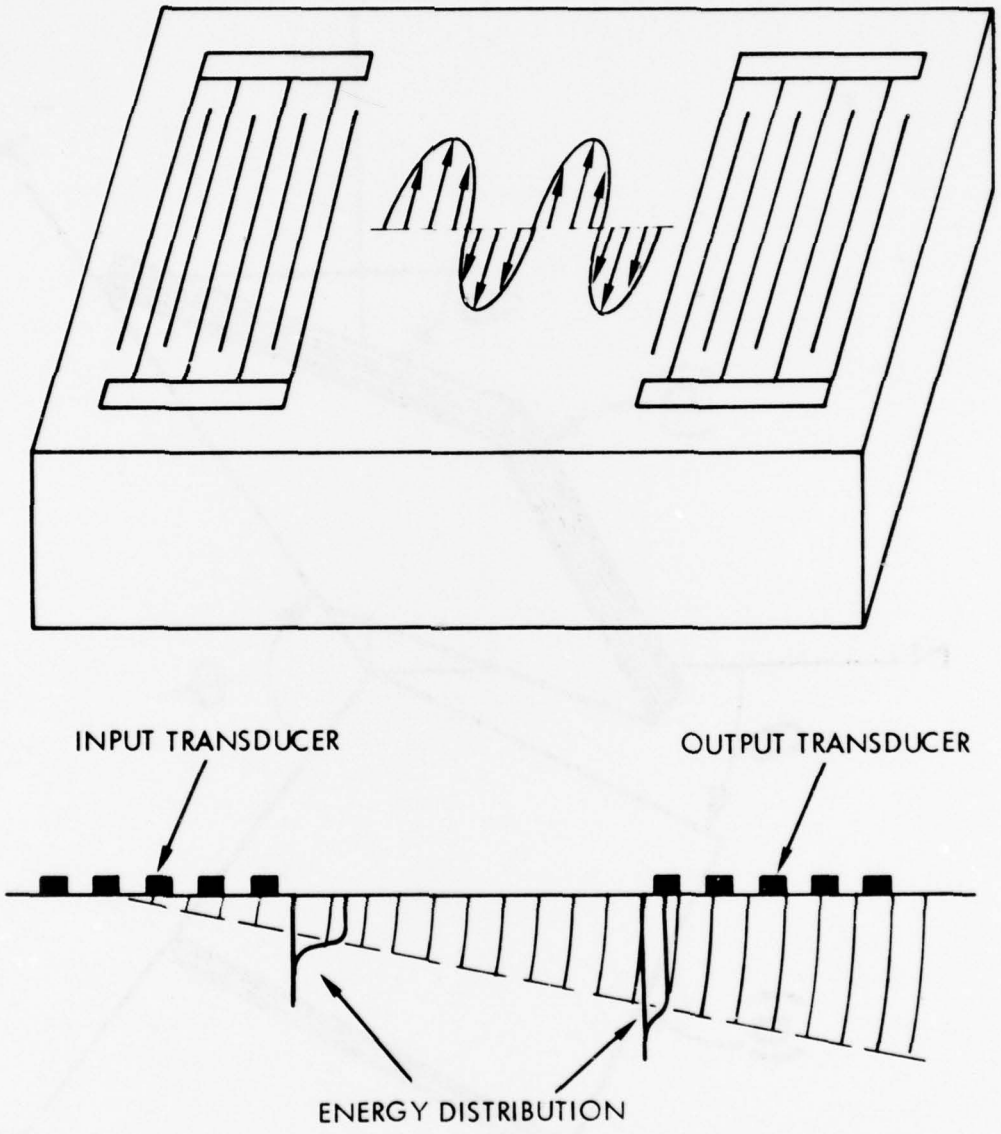


FIGURE 2. Schematic of SBAW Delay Line.

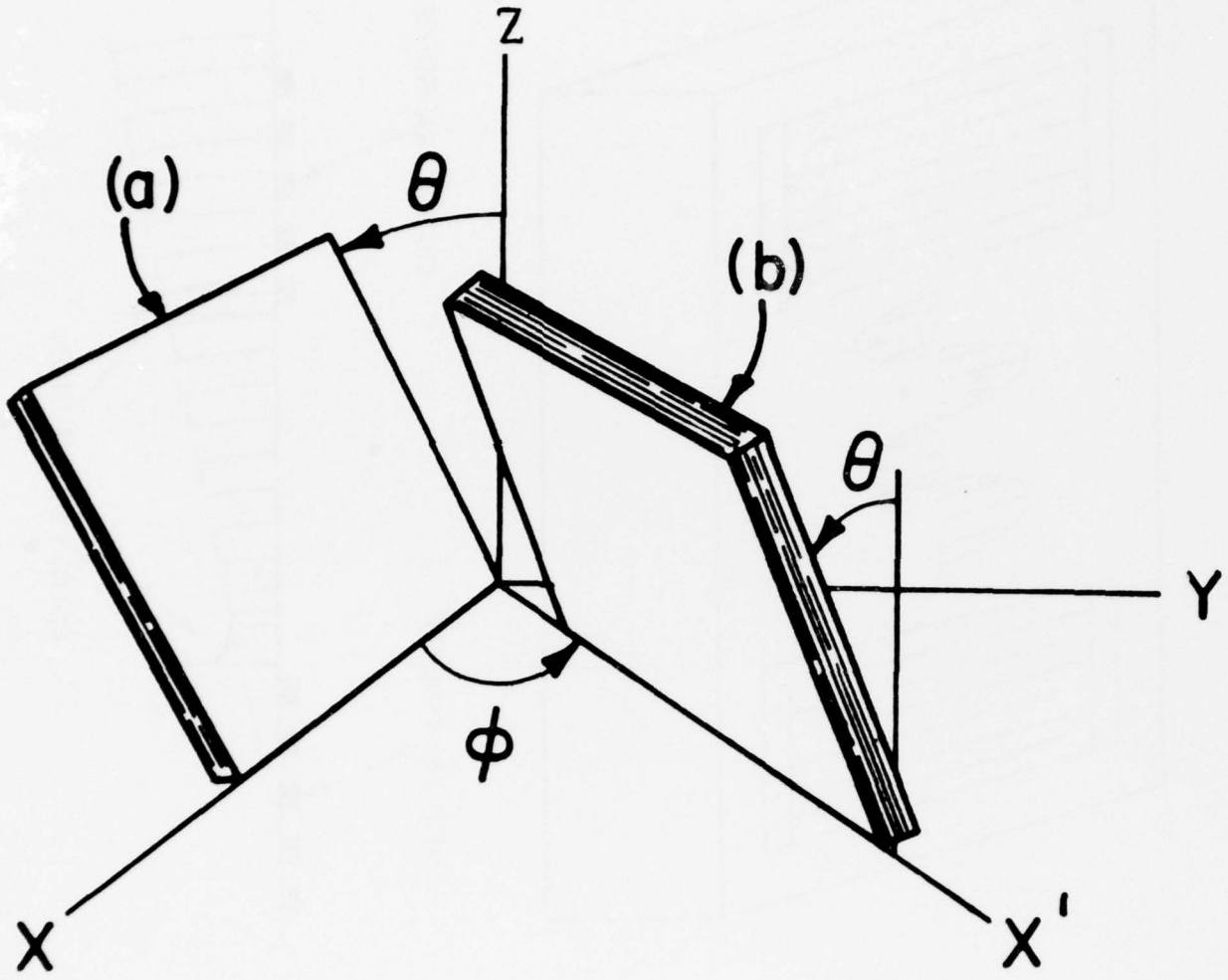


FIGURE 3. Singly (a) and Doubly (b) Rotated Plates.

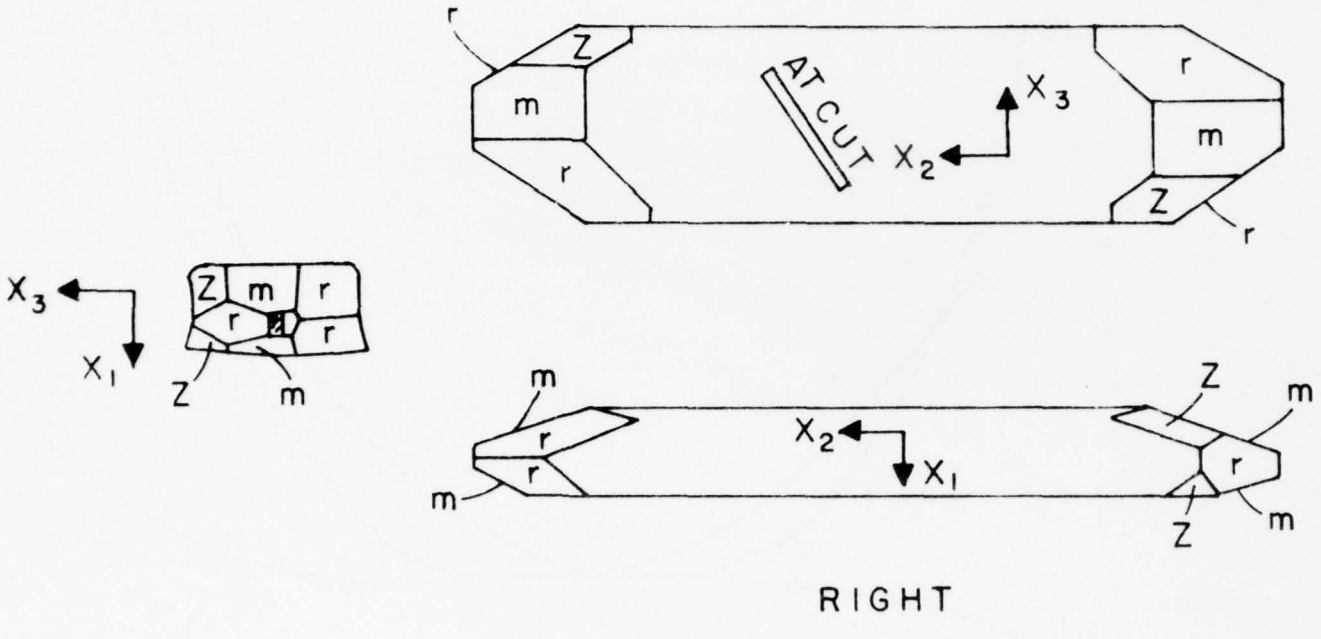


FIGURE 1. Cultured Bar of Right-Handed Quartz.

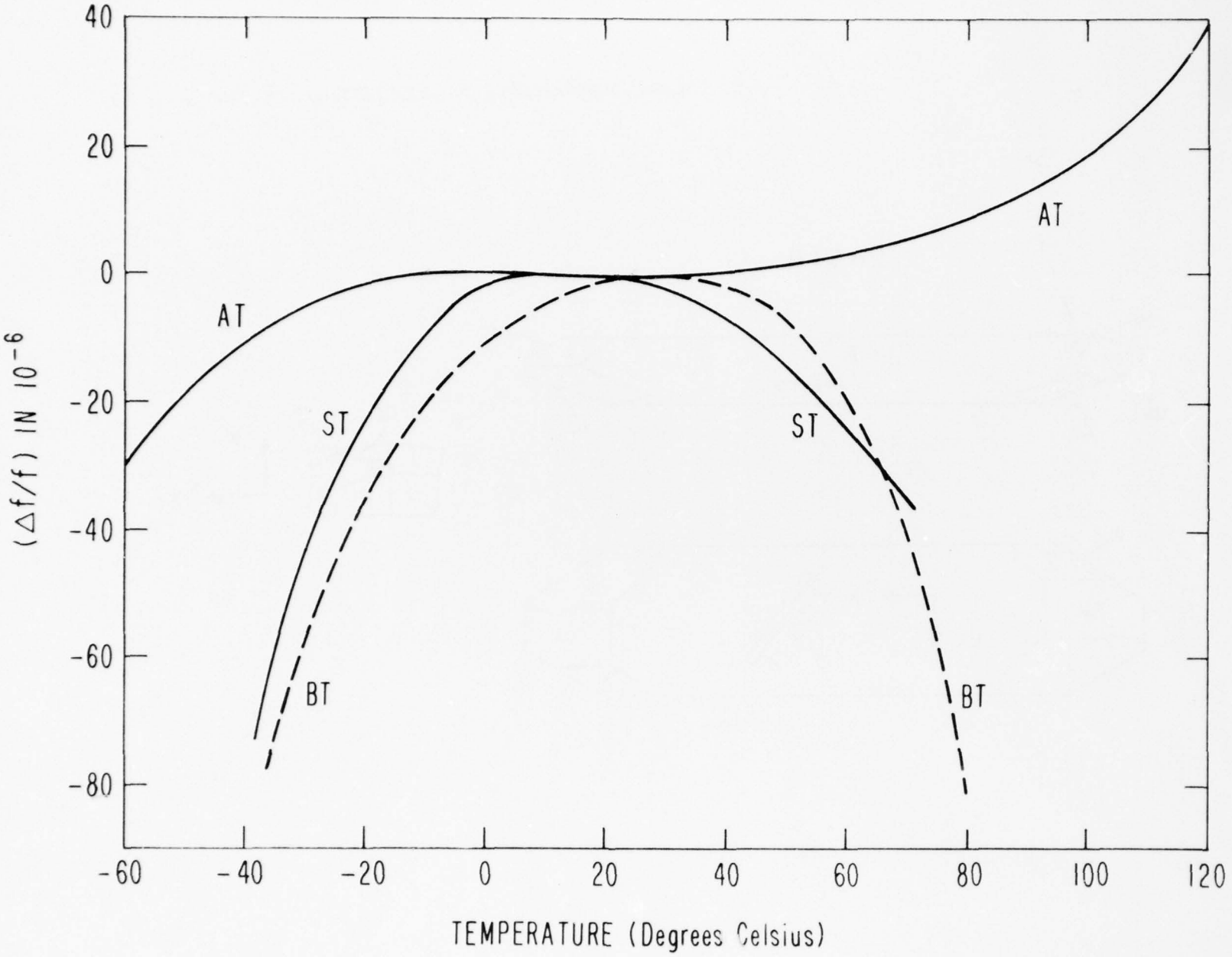


FIGURE 5. Frequency-Temperature Characteristics of Cuts.

When an ST cut, which normally supports SAWs propagating along $X_1$, has its IDT array turned by 90°, it produces SBAWs propagating along $X_3'$ (or Z'). The ST cut is nearly perpendicular to the BT cut, so the resulting SBAW has a frequency-temperature (f-T) characteristic very similar to that of the BT cut, because the BT has its BAW propagating in the thickness ($X_2'$) direction. As seen in Figure 5, these f-T curves are parabolic, and not as good as the cubic AT curve.

A big advantage of SBAWs on ST-cut quartz is that the frequency, for a given IDT, is about 1.6 times the corresponding SAW frequency. This ratio depends upon the angle θ, however, and decreases to nearly unity for the BT cut. The ratio can never be less than one because the limiting SAW velocity can never exceed the velocity of the slower shear wave propagating in the $X_1$ direction for rotated-Y-cuts. This velocity is $\sqrt{c_0/\rho}$, where

$$2c_0 = \left[ (c_{44} + c_{66}) - \sqrt{(c_{44} - c_{66})^2 + 4c_{14}^2} \right]. \qquad (1)$$

For SBAWs on BT-cut quartz, a compensating feature is the appearance of a cubic f-T characteristic, similar to that of the AT-cut. A family of curves near the BT-cut angle is shown for SBAW propagation in Figure 6; Figure 7 similarly shows the parabolic curves for propagation by SBAW on cuts situated about the AT-cut[13].

Another advantage of SBAWs over SAWs on singly rotated quartz is the absence of SAW generation. When the IDT is arranged for SAW propagation along $X_1$, BAWs are necessarily produced, as will be seen in a section below; but when propagation of SBAWs take place along $X_3'$, SAWs are not generated. This produces a very clean mode spectrum for SBAW devices.

Lewis[11,17] also investigated SBAWs on rotated-Y-cuts of lithium tantalate ($LiTaO_3$), but found that, although there was no coupling to SAWs in crystals of class 3m, all cuts of this family had bad TCs. Because of the very large piezoelectric coupling in lithium tantalate, it is useful in wideband filter applications despite its temperature behavior. Examples of this were shown by Kagiwada[23] for lithium tantalate and lithium niobate.

Based upon current work on singly rotated cuts supporting SBAWs, particularly on quartz, the key features summarized in Table 1 are now apparent. In Table 2 are given SBAW capabilities that have been demonstrated in the laboratory to date. It appears that devices based upon the SBAW principle may very well find significant applications as follows:

- delay lines
- resonators
- bandpass filters
- oscillators
- synthesizers

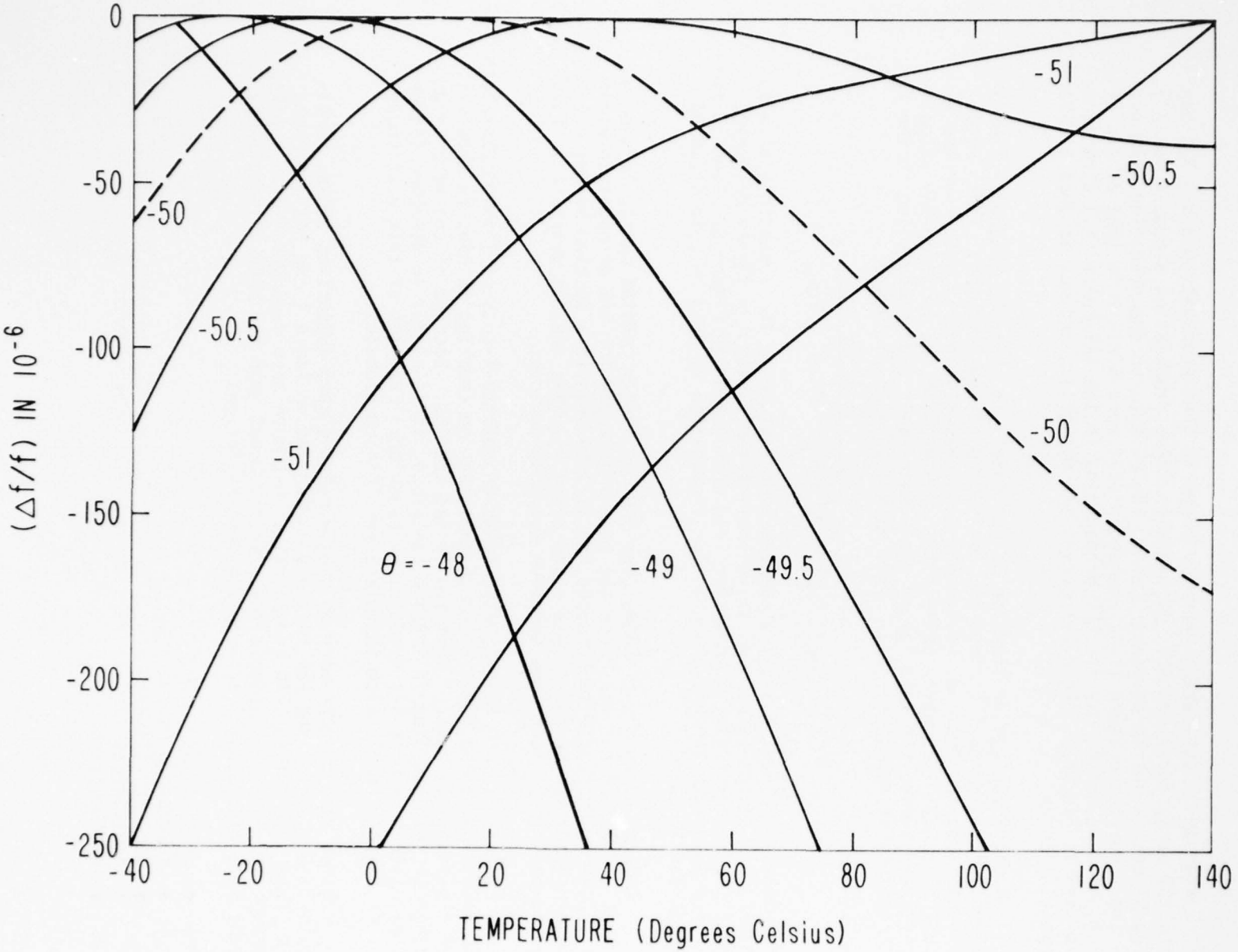


FIGURE 6. Frequency-Temperature Curves for BT-Cut Family.

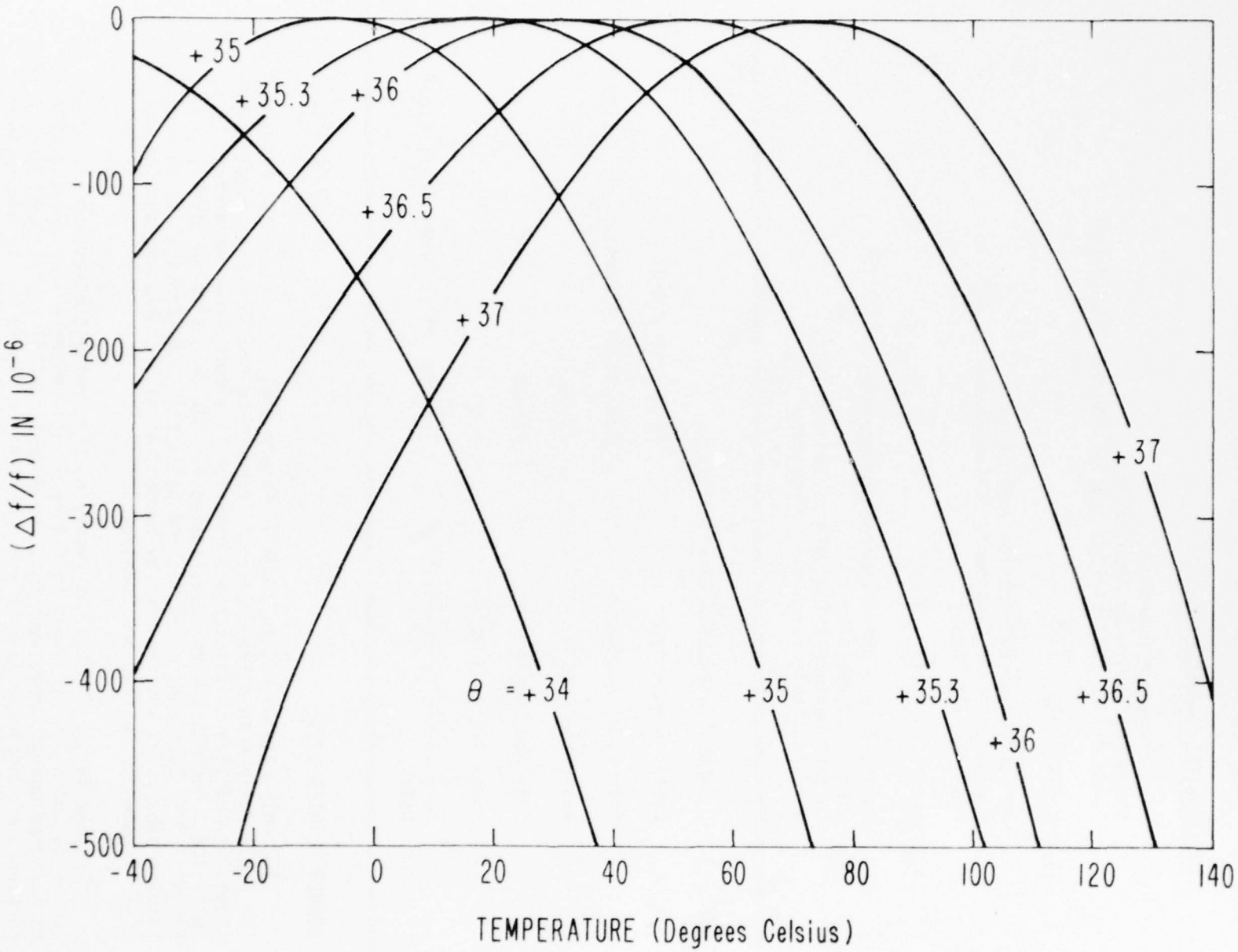


FIGURE 7. Frequency-Temperature Curves for AT-Cut Family.

TABLE 1. Key Features of Shallow Bulk Acoustic Waves

INTERDIGITAL TRANSDUCTION

High Frequency Operation
Response Shaping By Apodization
Large Design Flexibility; Spatial Fourier Transforms

PLANAR STRUCTURE

Semiconductor Fabrication Techniques
Microelectronic Components/IC-Compatable
Mechanically Rugged

PERFORMANCE POTENTIAL

Parabolic or Cubic Temperature Behavior
Clean Mode Spectrum
Surface Contamination/Defects Insensitivity
Wave Available for Signal Processing

TABLE 2. Demonstrated SBAW Capabilities

| | |
|---|---|
| Center Frequency | 60 MHz to 2.3 GHz |
| Fractional Bandwidth | 0.3% to 2% (Quartz); 15% ($LiTaO_3$) |
| Insertion Loss | 13 dB |
| Sidelobe Suppression | >55 dB |
| Shape Factor 3 dB/40 dB | 1.4 |
| Temperature Coefficient of Delay | Zero for First Order Coefficient |

DOUBLY ROTATED CUTS

A doubly rotated cut is shown in Figure 3(b). It is denoted (YXwℓ)Ø/θ. The angle Ø gives an extra degree of freedom and provides additional advantages; in addition to temperature behavior it allows other parameters to be optimized. Such cuts were investigated for BAW on quartz by Bokovoy and Baldwin[37-39], Bechmann, et al.[40], and Ballato[41]. SAW propagation on doubly rotated substrates was reported by Hauden, et al.[42]; SBAW propagation was briefly noted by Ballato and Lukaszek[43].

The BAW doubly rotated cut receiving the greatest attention at present is the SC cut[41]. It is shown in Figure 8 outlined on a line drawing of a bar of cultured quartz grown such that the Ø angle (≈22°) has already been incorporated. A photograph of such a bar is seen in Figure 9. In manufacture, only the θ angle (approximately that of the AT cut) need be critically adjusted.

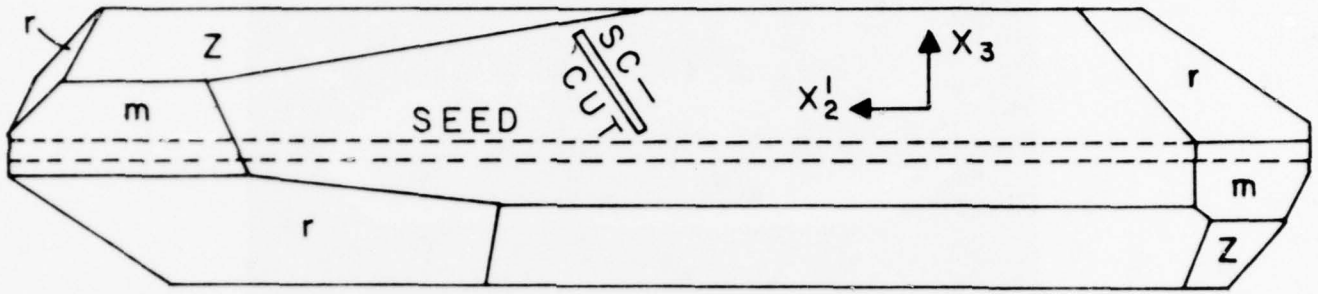


RIGHT — HANDED CULTURED QUARTZ

SC — BAR

FIGURE 8. Line Drawing of SC-Bar of Cultured Quartz.

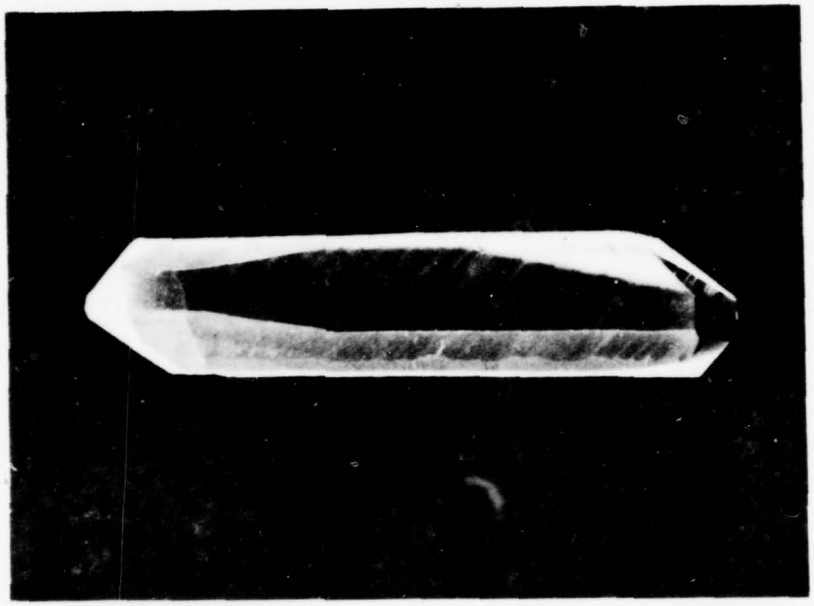

FIGURE 9. Photograph of SC-Bar of Cultured Quartz.

Figure 10 depicts a doubly rotated BAW plate with bulk wave propagation shown taking place in the thickness direction. A SBAW plate is shown adjacent. The propagation direction for the SBAW is shown between the IDTs to be along $X_1''$, i.e., parallel to the BAW propagation direction. This leads to a simple receipt whereby already-known results for doubly rotated BAW plates can be used to determine the approximate behavior of the "corresponding" SBAW plate. From the figure it is seen that the plate that corresponds to the $(YXw\ell)\phi/\theta$ BAW plate is a plate of orientation $(YXw\ell w)\phi/(\theta\pm90^{\circ})/\psi$. Notice that $\phi$ is the same for both plates. Also notice that $\theta$ need only be replaced by $\theta\pm90^{\circ}$ (keeping the result in the range $|\theta| \leq 90^{\circ}$).

It will be further seen that the rotational symbol of the SBAW plate describes a triply rotated cut. The third angle, given as $\psi$ in Figure 10 permits the specification of a whole family of SBAW plates for each corresponding BAW plate, allowing one to optimize some parameter of operation such as temperature coefficient, coupling factor or beam steering angle. Because the SBAW mode most adapted to satisfying the traction-free boundary conditions on the crystal surface is the horizontally polarized shear mode, $\psi$ can be chosen so that the $X_1'' - X_2''$ surface is along the direction given by the particle motion for one of the shear waves propagating along $X_2''$ in an unbounded medium. This enhances the ease with which the mode can propagate, and the cleanliness of the resulting mode spectrum.

The triply rotated cut angles $\phi/\theta/\psi$ can be reduced readily to an equivalent doubly rotated set by the formulas of spherical trigonometry; doubly rotated plates are the most general type of cut.

The doubly rotated BAW cuts in quartz have been mapped for f-T behavior in the entire $\phi/\theta$ plane[40]. An altitude chart of the first-order temperature coefficient frequency for the slower shear mode (the so-called c-mode) is given in Figure 11. This quantity corresponds to the slope of the f-T curves in Figure 5 at room temperature. By changing the ordinate scale from $\theta$ to $(\theta \pm 90^{\circ})$ one has the TC altitude chart, in first approximation, for doubly rotated SBAW plates for the slow-shear mode. Figure 12 gives the altitude chart for the faster shear mode (b-mode).

In general, all three of the wave types that exist for plane wave propagation in an unbounded medium exist and propagate in an SBAW plate, although their properties are modified by the finite boundaries. The quasi-longitudinal ("a" mode), and the two quasi-shear waves ("b", and "c" modes) are shown by their spectrographic responses for a plate $(YXw\ell)\phi=10^{\circ}/\theta=+34^{\circ}$ in Figure 13. Here the faster shear wave ("b" mode) is more strongly driven, because of its higher piezoelectric coupling, and also because its motion more nearly coincides with the direction of the surface of the plate, than the slower ("c") mode. By calculating the properties of a BAW plate having $\phi = 10^{\circ}$ and $\theta = -54^{\circ}$ one may get an approximate idea of the parameters of SBAW propagation in the $\theta = +34^{\circ}$ plate. Some of these are shown in Table 3. The top row gives the frequency constant N (one half the acoustic wave velocity); the second row gives the piezoelectric coupling for BAW propagation; the first order TC of frequency is shown in row three, and the calculated frequency response of a particular IDT is given in the last row. The mode strengths and frequencies are to be compared with those in Figure 13, where it is seen that the agreement is quite good. In Figures 14, 15, and 16 are given curves of N (the frequency constant), $|k|$ (the piezoelectric coupling), and $T_f$ (the first order TC of frequency) for quartz BAW propagation for cuts $(YXw\ell)$ $\phi = 0^{\circ}(6^{\circ})\ 30^{\circ}/\theta$.

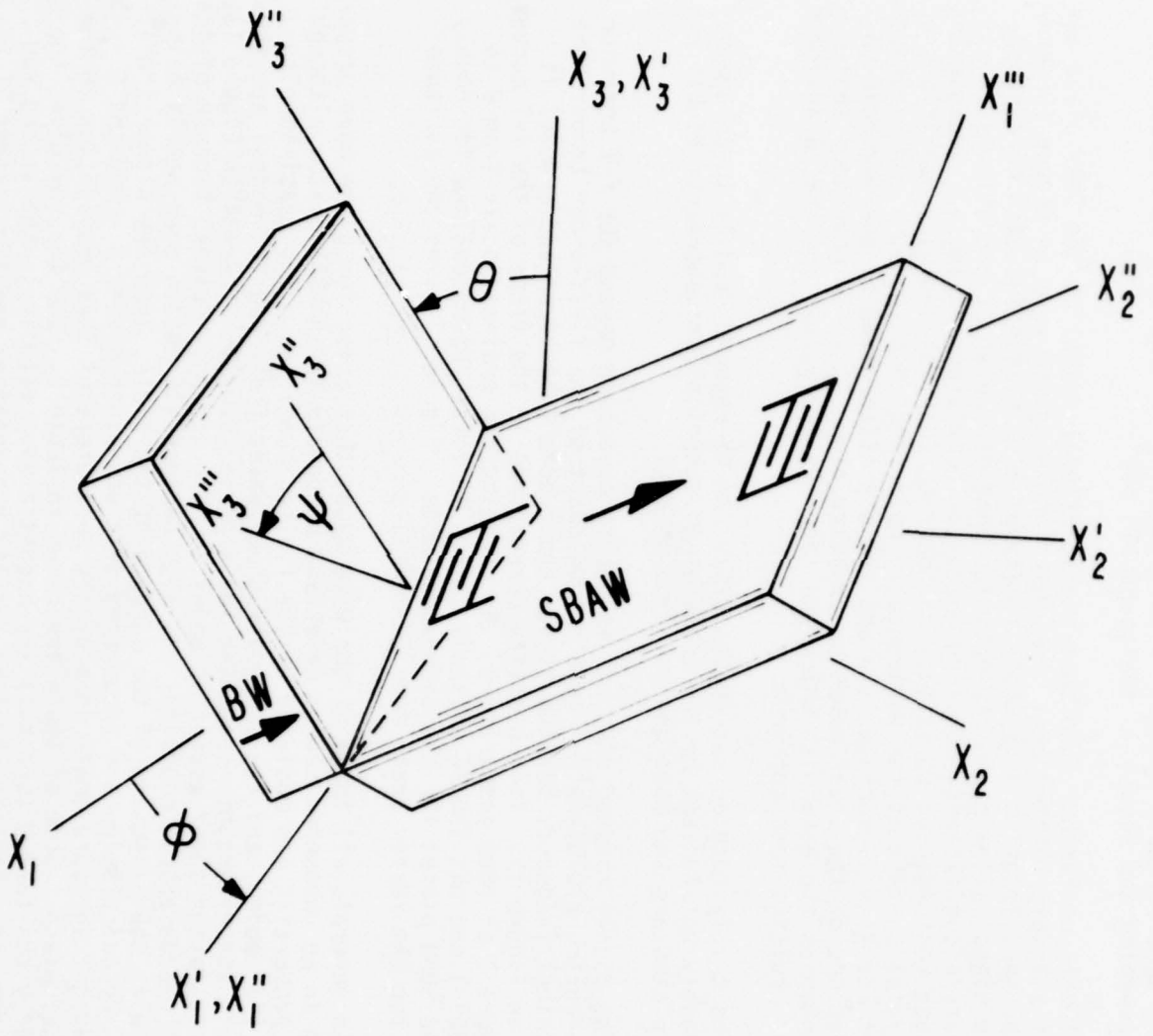


FIGURE 10. Doubly Rotated BAW and Triply-Rotated SBAW Plates.

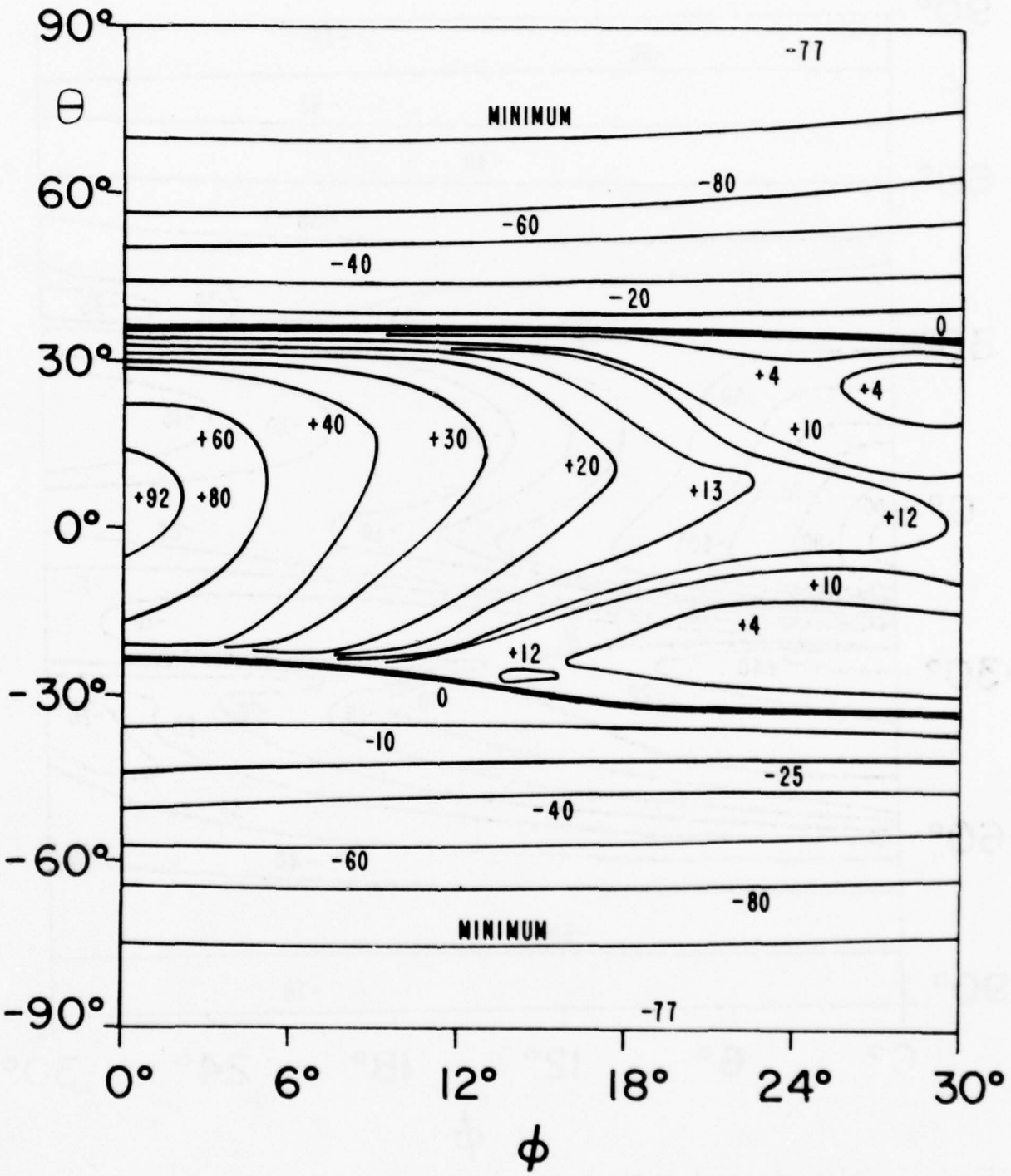


FIGURE 11. Altitude Chart of $T_f$ (mode c) in Quartz.

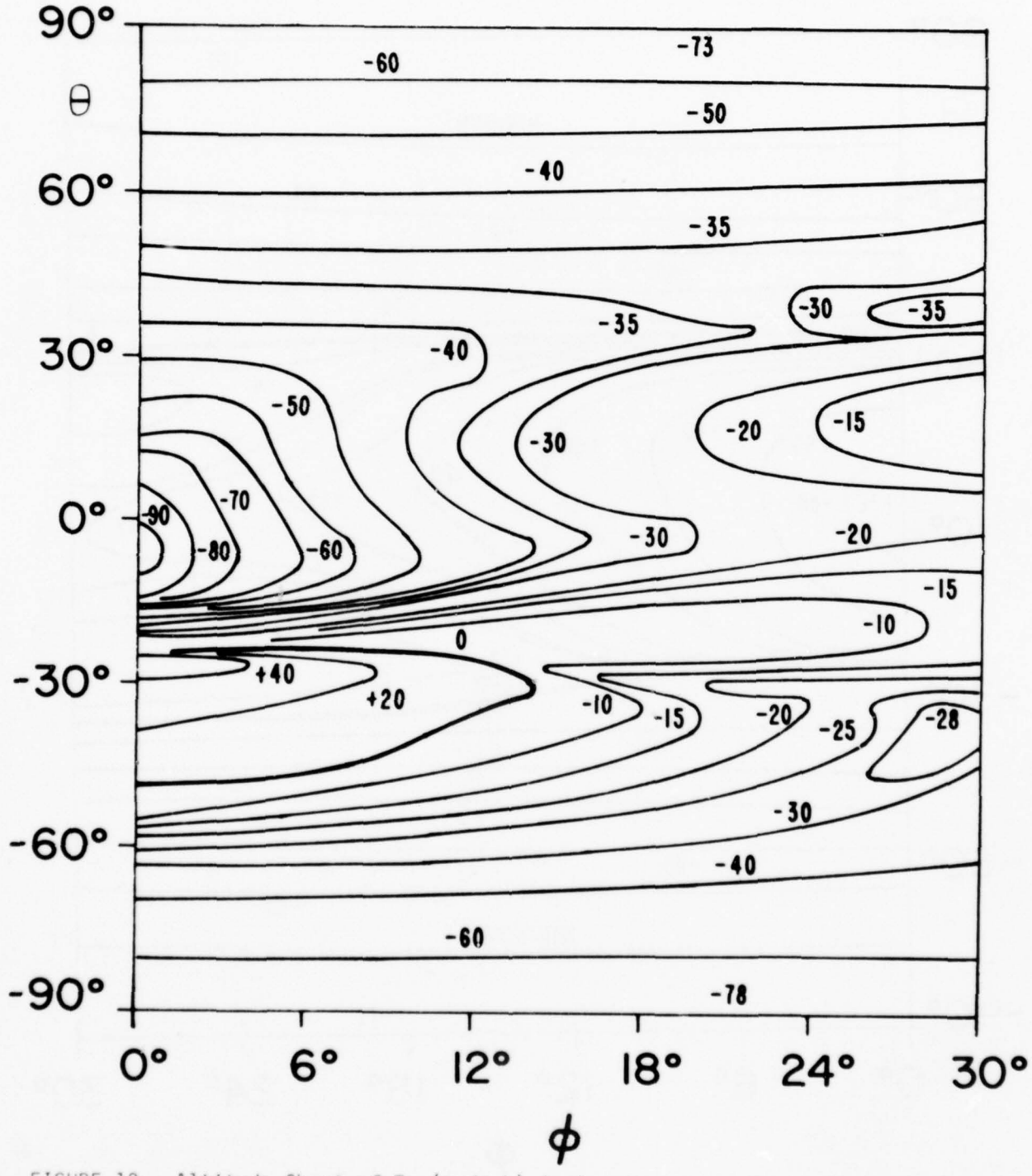


FIGURE 12. Altitude Chart of $T_f$ (mode b) in Quartz.

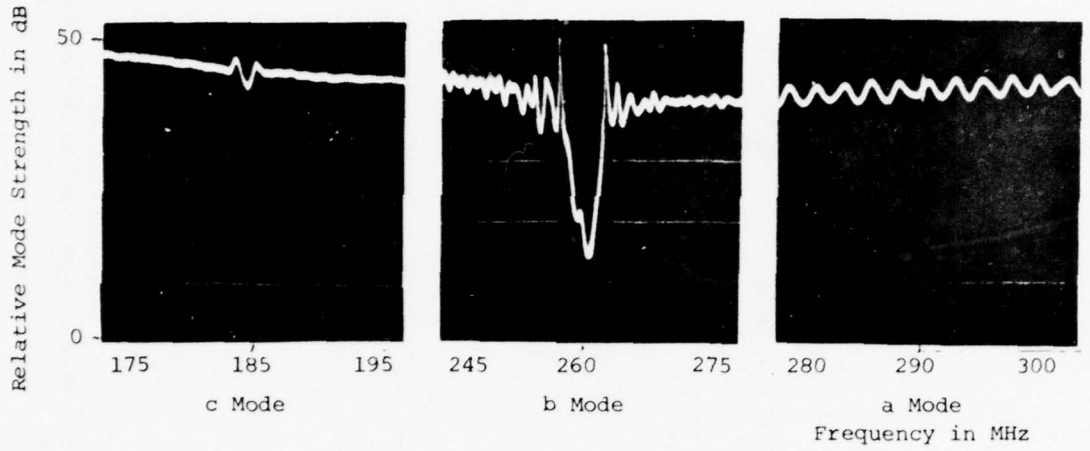


SBAW MODE SPECTROGRAPH OF DOUBLY ROTATED QUARTZ PLATE.

FIGURE 13. Spectrographs of Three SBAW Modes.

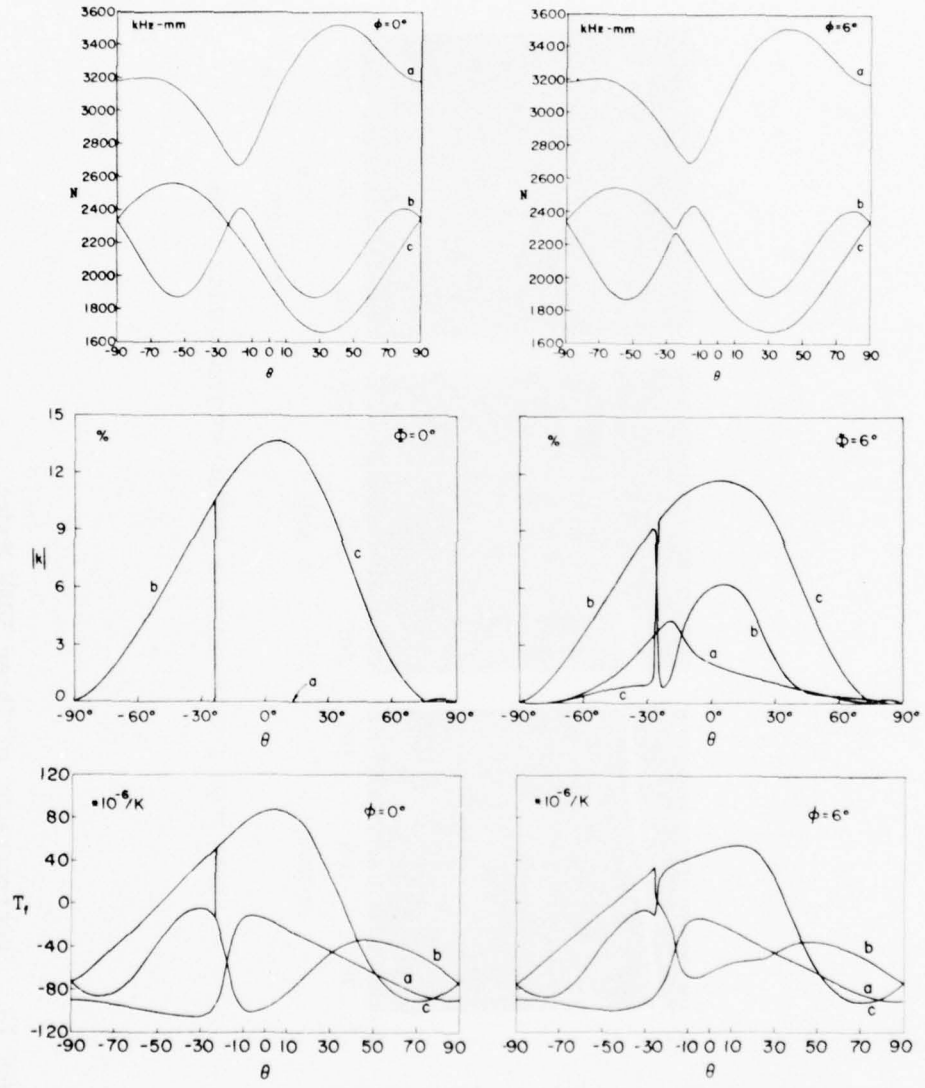


FIGURE 14. N, |k|, and $T_f$ for (YXωt)0°, 6°/θ Quartz Cuts.

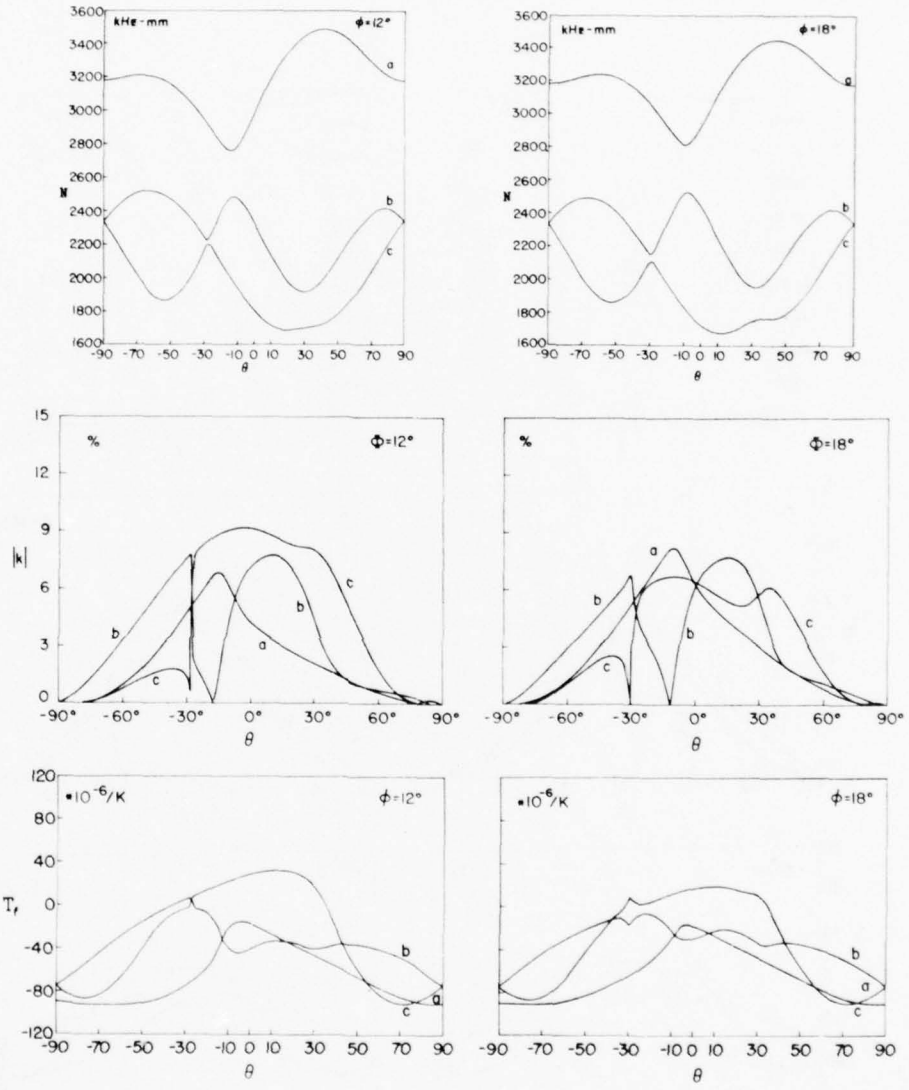


FIGURE 15. N, |k|, and $T_f$ for (YXωΦ)12°, 18°/θ Quartz Cuts.

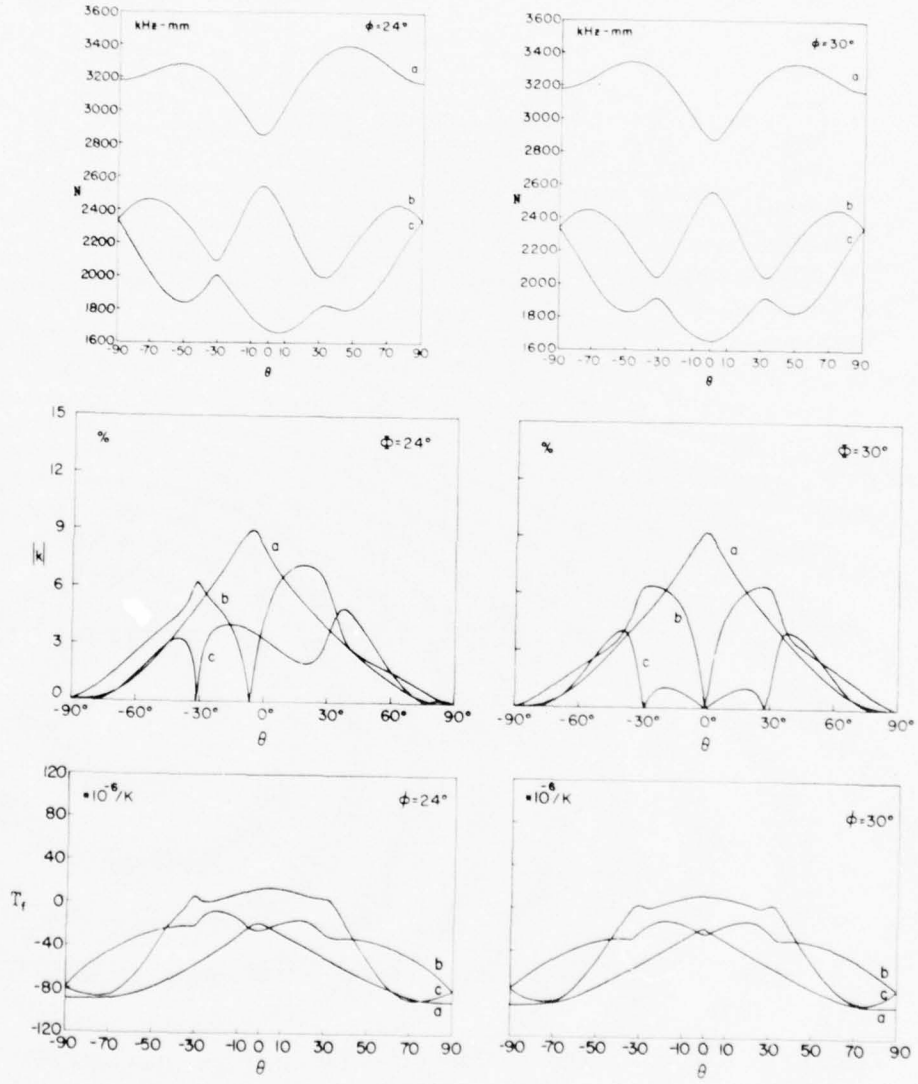


FIGURE 16. N, |k|, and $T_f$ for (YXw)24°, 30°/θ Quartz Cuts.

TABLE 3. Shallow Bulk Acoustic Mode Properties

$(YXw\ell)$ $\phi = 10^{o}$ / $\theta = +34^{o}$; Z-Propagation SBAW

| | MODE c | MODE b | MODE a |
|---|---|---|---|
| N (m/s) | 1873 | 2521 | 3177 |
| (K) % | 0.78 | 3.77 | 1.04 |
| $T_f$ ($10^{-6}$/K) | -56.0 | -20.2 | -94.6 |
| f(MHz) | 185.3 | 249.4 | 314.3 |

Certain orientations in quartz should be avoided. These include BAW plates (and their corresponding SBAW cuts) of orientations near $\phi=0^{o}$, $\theta \simeq -24^{o}$ and $\phi \simeq 10.4^{o}$, $\theta \simeq -26.6^{o}$. Both of these directions are directions of degeneracy, where the two shear velocities coincide; near these points the energy flux deviations are large.

PIEZOELECTRIC TRANSDUCTION

Transduction of acoustic waves via the piezoelectric effect may be determined if the forces produced are known. The force densities are given by the stress-gradients, which, in turn, are brought about by the electric fields produced by the IDT array[44]. The piezoelectric portion of the mechanical stress relation is

$$T_{ij} = - e_{kij} E_k \ . \qquad (2)$$

The mechanical force-densities $F_j$ are then

$$F_j = - e_{kij} E_{k,i} \ . \qquad (3)$$

IDT fingers produce electric fields $E_k$ that are very sharply peaked at the electrode edges. An example is given in Figure 17, where is shown the static field parallel to, and at, the crystal surface, normalized to the field that would exist between parallel plate capacitors of equal gap; the field possesses branch-point singularities at each edge. The other field components behave in a similar manner. Because of the spikes in $E_k$, the force densities can be represented, to an excellent approximation as delta-functions, and the excitation of acoustic waves evaluated in a straightforward manner[45].

Taking as an example a rotated-Y-cut of quartz of orientation $(YX\ell)\theta$, with an IDT array along $X_1$, the electric field gradients peak sharply at the electrode finger edges, and are $E_{1,1}$ (largest) and $E_{2,2}$ plus both $E_{2,1}$ and $E_{1,2}$. The rotated piezoelectric constants that are non-zero are $e'_{111}(=e_{111})$, $e'_{122}$, $e'_{133}$, $e'_{123}$, $e'_{213}$, $e'_{212}$, $e'_{313}$, and $e'_{312}$. Therefore $E_{1,1}$ produces

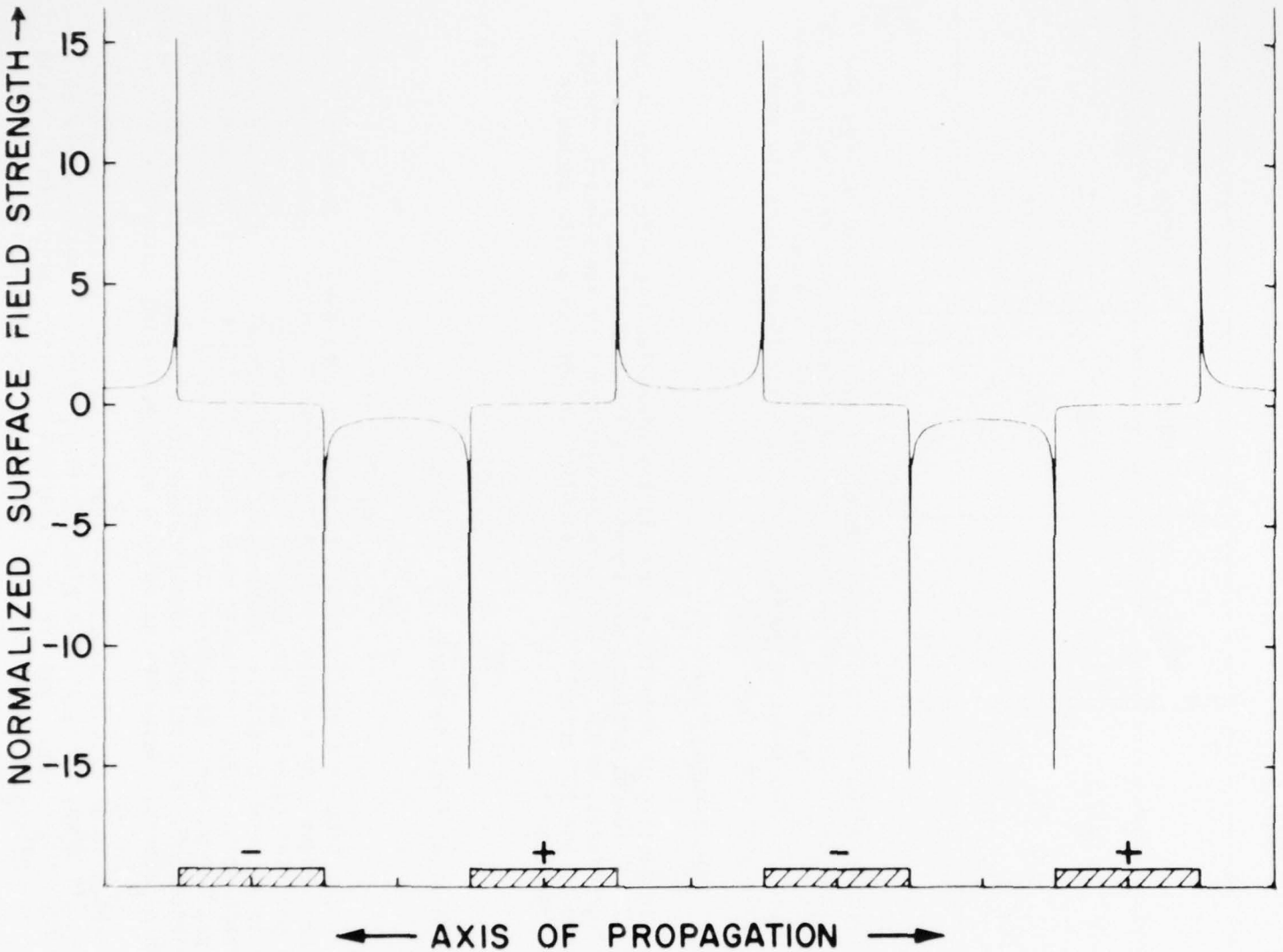


FIGURE 17. Static Electric Field Distribution for IDTs.

$X_1$ directed forces, but no forces along $X_2$ or $X_3$. $E_{2,2}$ likewise generates $X_1$ forces. The weaker gradients $E_{2,1}$ and $E_{1,2}$ both produce $X_3$ and $X_2$ forces. The $X_1$ and $X_2$ forces lead to SAWs.

If the IDT array is rotated so that the finger edges are parallel to the $X_1$ axis and propagation takes place along $X_3$, then $E_1$ vanishes, along with the gradients $E_{2,1}$ and $E_{3,1}$. The gradients $E_{2,2}$; $E_{2,3}$; $E_{3,2}$ and $E_{3,3}$ all produce forces directed along $X_1$ but no other component of force. SAW propagation cannot take place but an SH-type of BAW propagates, and this is the SBAW that has been investigated to date.

A similar calculation shows that for rotated-X-cuts of crystals in class 32 (quartz, aluminum phosphate), SBAW propagation along any direction parallel to the free surface produces SAW generation as well. Again, for rotated-X-cuts of class 3m, both SBAW and SAW are generated for any propagation direction parallel to the plate surface.

It appears, then, that a rather elementary consideration based on the piezoelectric relations and the delta-functions produced by the IDT array yields valuable insight into the production of acoustic waves in piezo crystals. This approach can readily be placed on a quantitative basis. Another result of the delta-function model of transduction is the realization of SAW and SBAW equivalent circuits in the analog form shown in Figure 18. The piezo-transformers are placed at the locations of the electrode edges. Unattached electrodes are simply left unconnected to the supply voltage.

## TRAPPING/DUCTING

Energy trapping was applied to BAW plates by Mortley[46-49], Shockley, et al.[50,51], and Mindlin[52]. Trapping or ducting of SAWs has been treated by Oliner[53], Ash, et al.[54], and Tiersten, et al.[55-57]. It was suggested for SBAW by Lewis[13], and experimentally proven by Kagiwada, et al.[23,26].

The periodic perturbations resulting from the unconnected metallic electrodes placed in the SBAW path produce the ducting effect by a combination of mass-loading and piezoelectric effects. The SBAW wave becomes analogous to a Love wave - a horizontally polarized shear wave that requires a discontinuity or material gradient in the depth direction for propagation.

For untrapped SBAW propagation, the transmission lines in Figure 18 are non-uniform in their characteristic impedance and propagation wavenumber; the use of a ducting structure renders the lines uniform.

In Figure 19 is shown an energy-trapped SBAW narrow-band filter on ST-cut quartz[26]. It is seen how extremely clean the mode spectrum is, resulting from the absence of SAWs; this is further borne out by the broad frequency sweep of the same filter[24] shown in Figure 20.

## RADIATION FIELD

SBAW radiation patterns have been very successfully calculated on the basis of simple antenna theory by Lewis[13,58], and on the basis of more extensive calculations by Jhunjhunwala, et al.[31], and Lee[32]. Results of an exact calculation for the rotated-Y-cuts of quartz excited by a single infinite line source are given by Kagiwada, et al., and are shown in Figure 21 for the

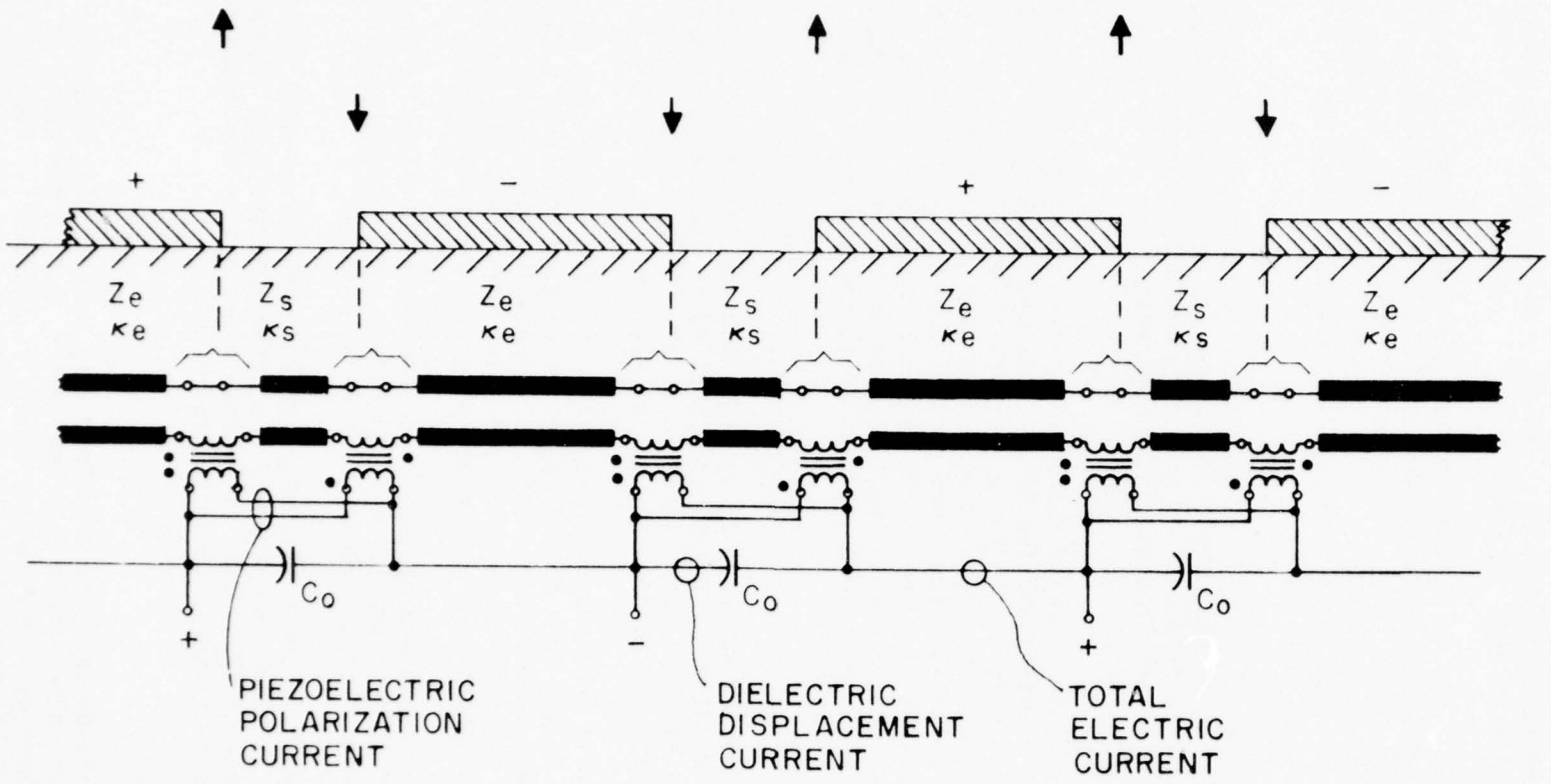


FIGURE 18. Equivalent Network for SBAW Transmission.

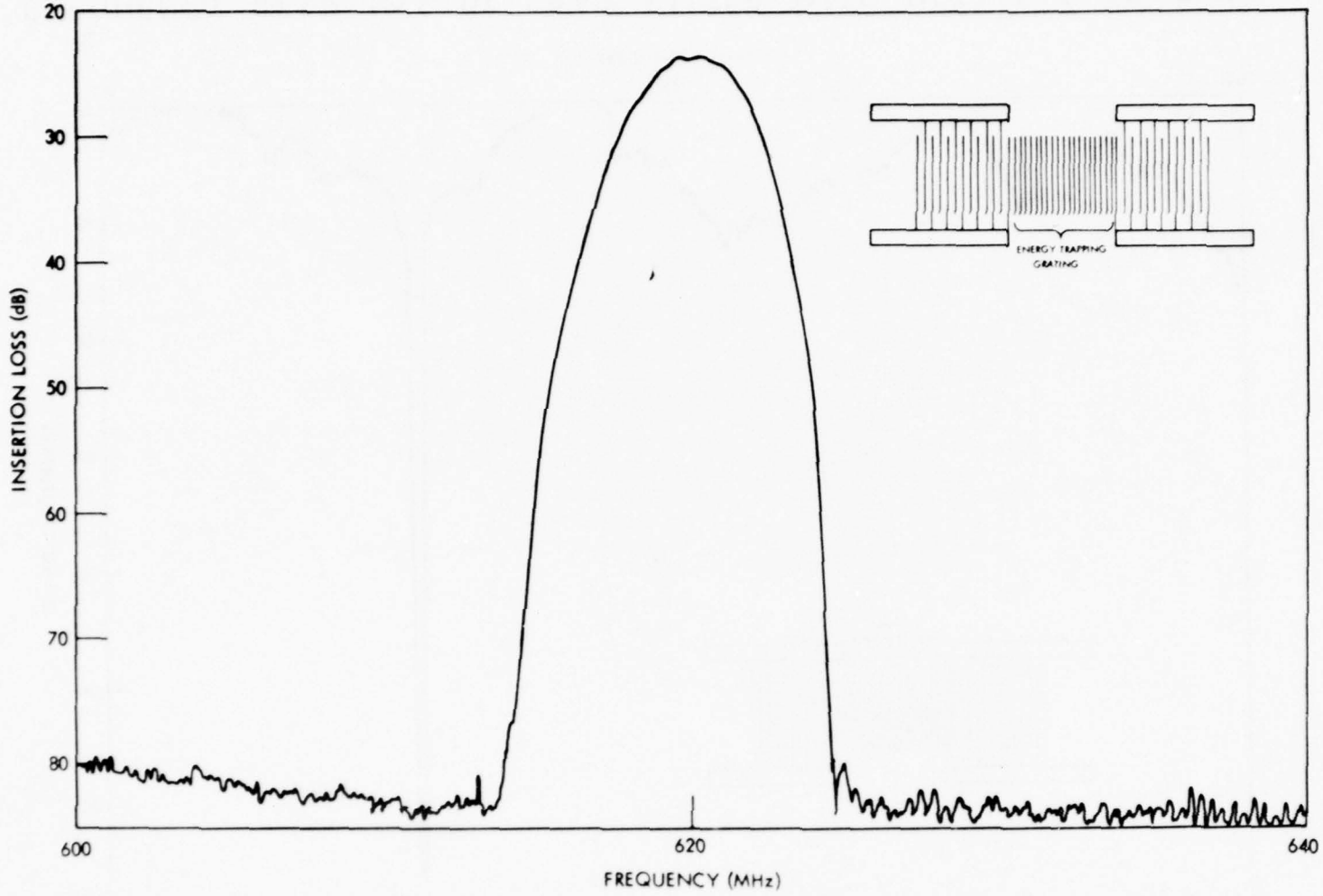


FIGURE 19. Narrowband Response of Bandpass SBAW Filter.

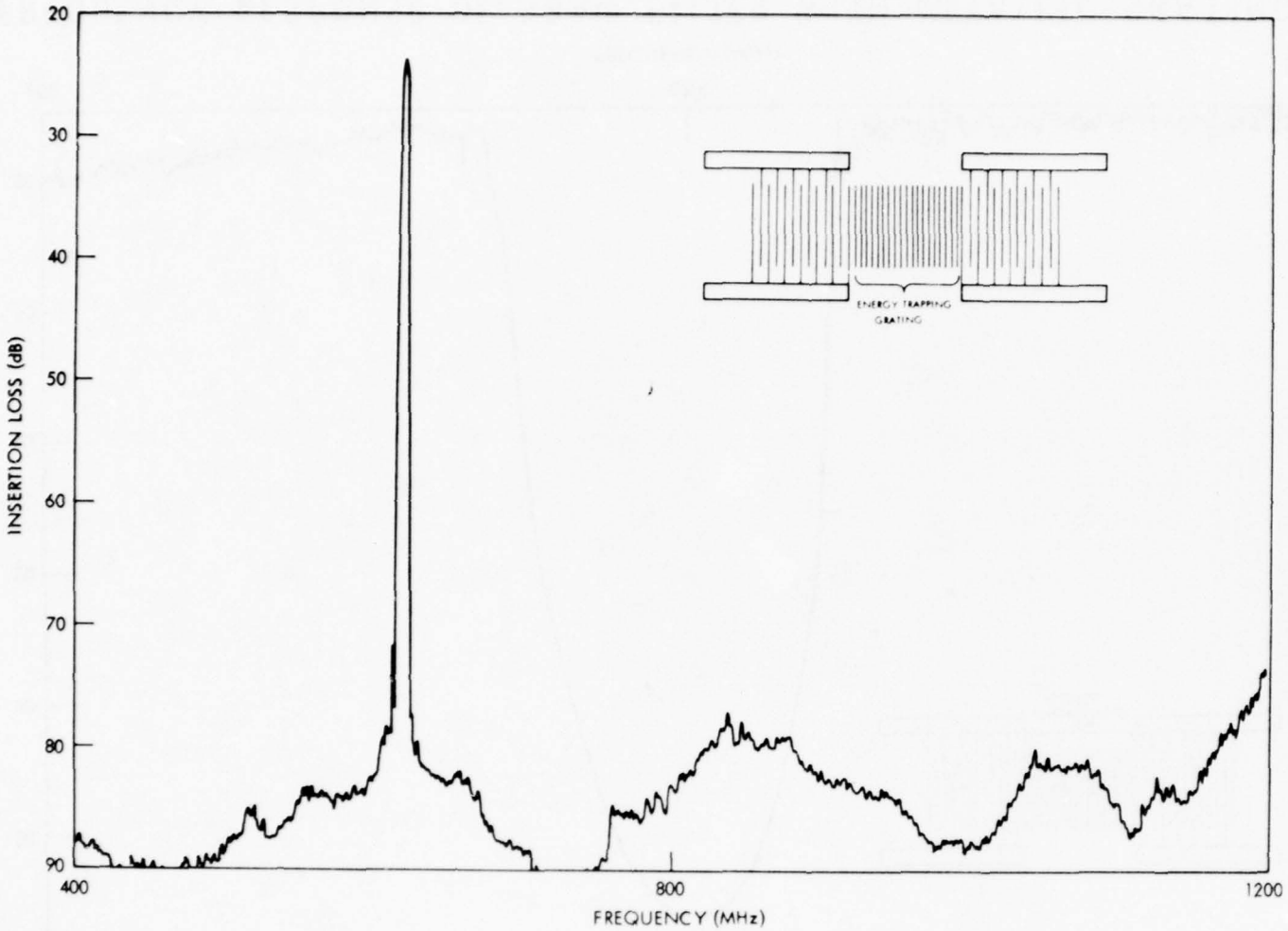


FIGURE 20. Wideband Response of Bandpass SBAW Filter.

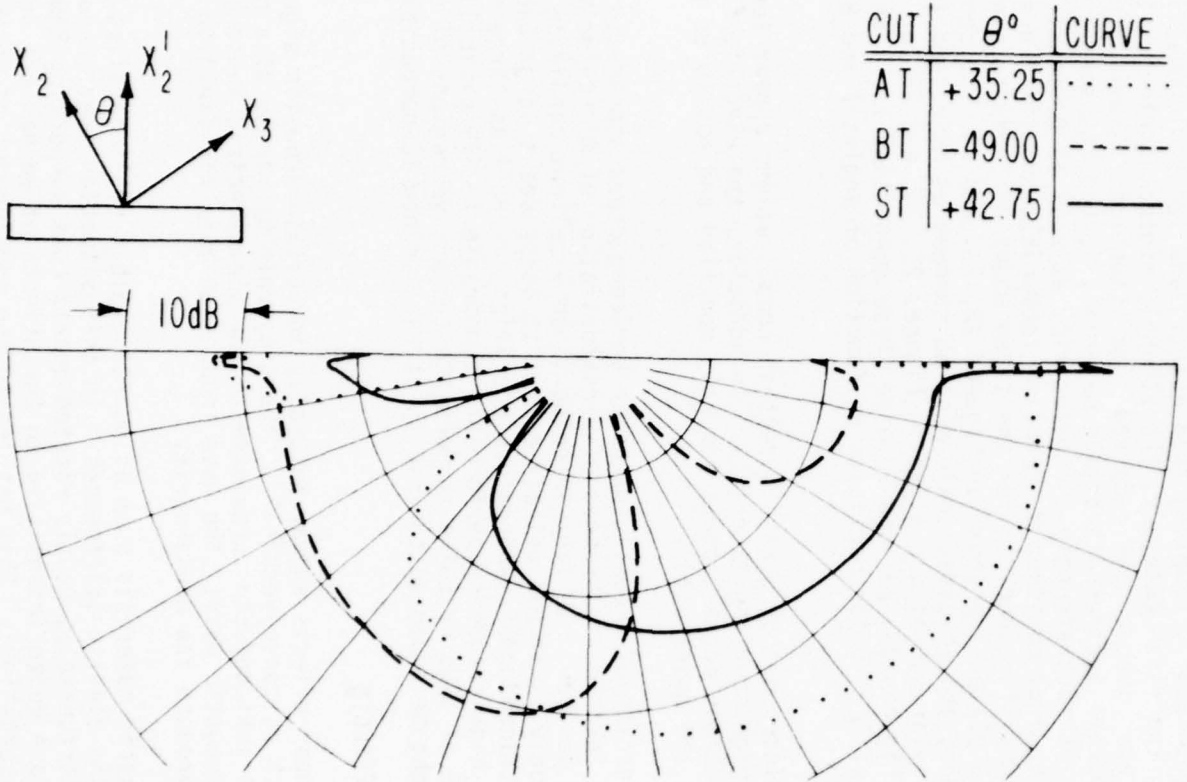


FIGURE 21. Far-Field Radiation Pattern of SBAW on (YXℓ)θ Quartz.

AT, BT, and ST cuts[27]. The plots are of relative radiated power in the far field. It is seen how dramatically the pattern varies with θ even between the adjacent AT and ST cuts. Further work will possibly make use of Z-transforms[59-61], modified to account for the anisotropy of the medium, to predict accurately the radiation from IDTs.

## NEW MATERIALS

Two areas of future device potential appear to be (1) materials with higher piezoelectric coupling than quartz, and (2) semiconducting piezoelectrics. In the first category, the strongly piezoelectric substances lithium tantalate and niobate have received some attention. Aluminum phosphate (berlinite) appears another attractive material; it has the same crystal class as quartz but is more strongly piezoelectric, as well as possessing a zero TC locus. Frequency constant N, coupling factor $|k|$, and first order temperature coefficient of frequency $T_f$ for the three modes of infinite singly and doubly rotated BAW plates are shown in Figures 22, 23, and 24. To convert to SBAW orientations, the abscissa scale must be changed as discussed in prior sections. Similar curves are given in Figures 25, 26, and 27 for lithium tantalate, and Figures 28, 29, and 30 give these quantities for lithium niobate. The locus of $T_f = 0$ for berlinite as function of angles Ø and θ is given in Figure 31.

As pointed out by Lewis[16], certain complications appear for SBAW propagation in high coupling materials. In addition, the electric field pattern at the electrode edges becomes strongly modified and has to be taken into account in the model used[45].

Propagation of acoustic waves in semiconductors appears to be an attractive way to further the process of miniaturization of microelectronic signal processing devices. Gallium arsenide is an excellent candidate material because not only is it piezoelectric, but it possesses a large bandgap, allowing high semiconductor temperature operation, as well as large mobility values, leading to high frequency performance comparable to SAW capabilities. Using the passage of SAWs or SBAWs to modulate the active regions of semiconductor devices might be expected to lead to attractive new IC-compatible devices.

## NONLINEAR EFFECTS

Nonlinear effects appear naturally in certain acoustic signal processing devices such as convolvers[62,63]. These operate by virtue of a nonlinear effect in the semiconductor proximate to the piezoelectric substrate that supports the acoustic wave; the wave induces an electric field in the semiconductor to produce the nonlinearity.

Dielectric materials such as quartz exhibit nonlinearities as well, primarily in the elastic stiffnesses. In this situation they are usually undesirable. Fortunately, doubly rotated quartz cuts supporting BAWs have been found that are quite insensitive to the effects of mechanical stress effects of various sorts[41,64]. This has led to the development of resonators that have very good resistance to mechanical shocks and electrode film stress changes. Closely related to this problem is that of frequency changes in BAW resonators due to abrupt temperature changes. Once again, doubly rotated quartz cuts have been found where this nonlinear elastic effect is minimized[65].

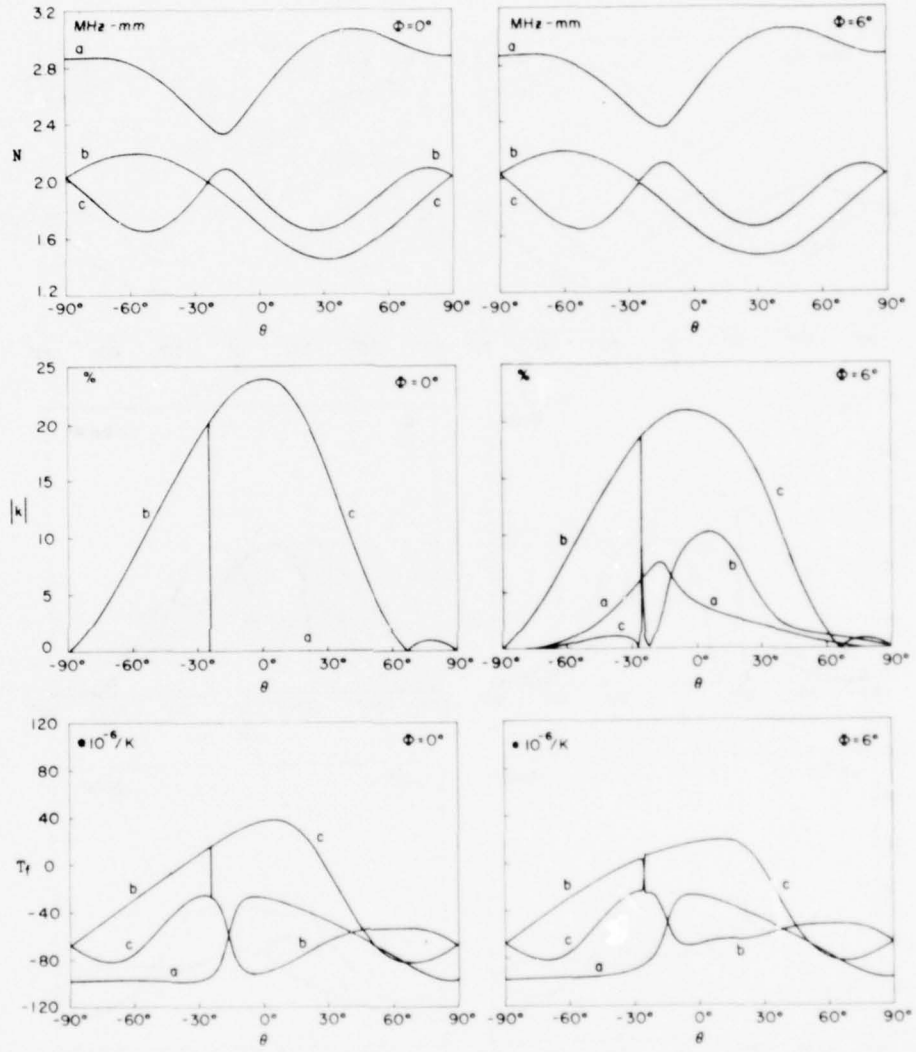


FIGURE 22. N |k|, and $T_f$ for (YXωℓ)0°, 6°/θ Berlinite Cuts.

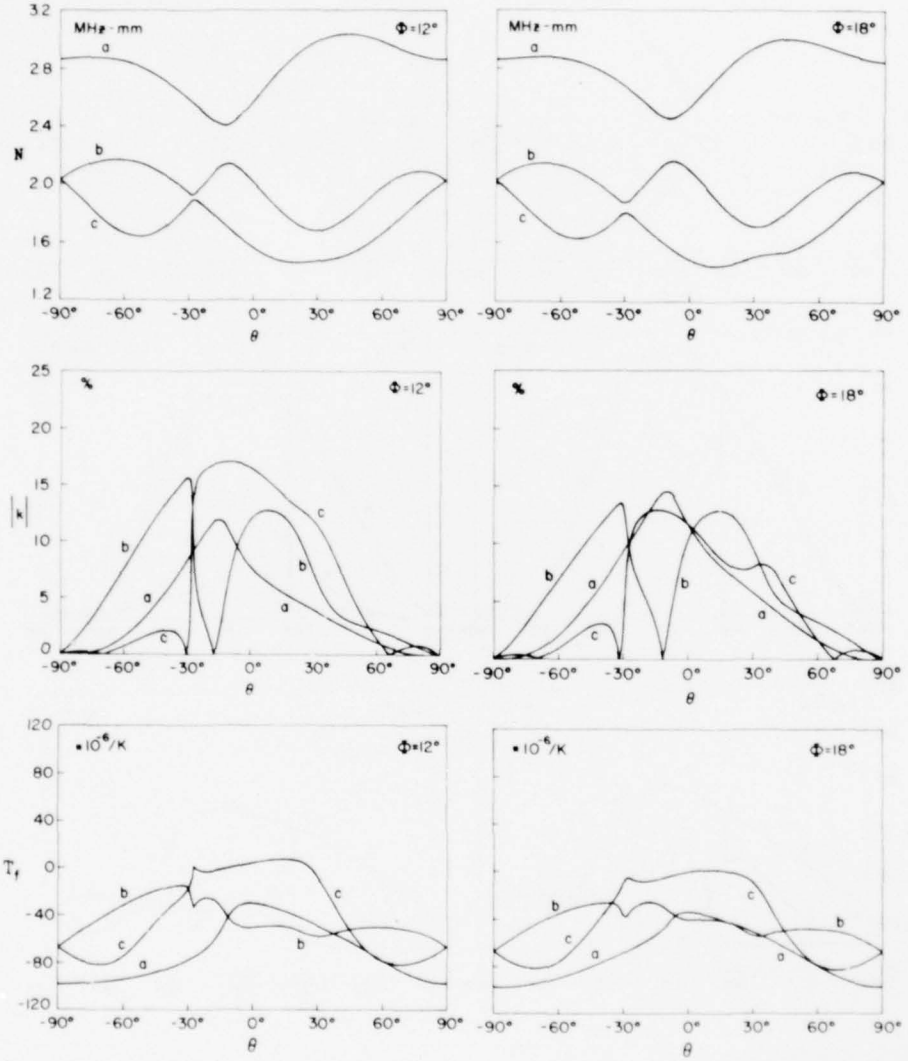


FIGURE 23. N, |k|, and $T_f$ for (YXω℄)12°, 18°/θ Berlinite Cuts.

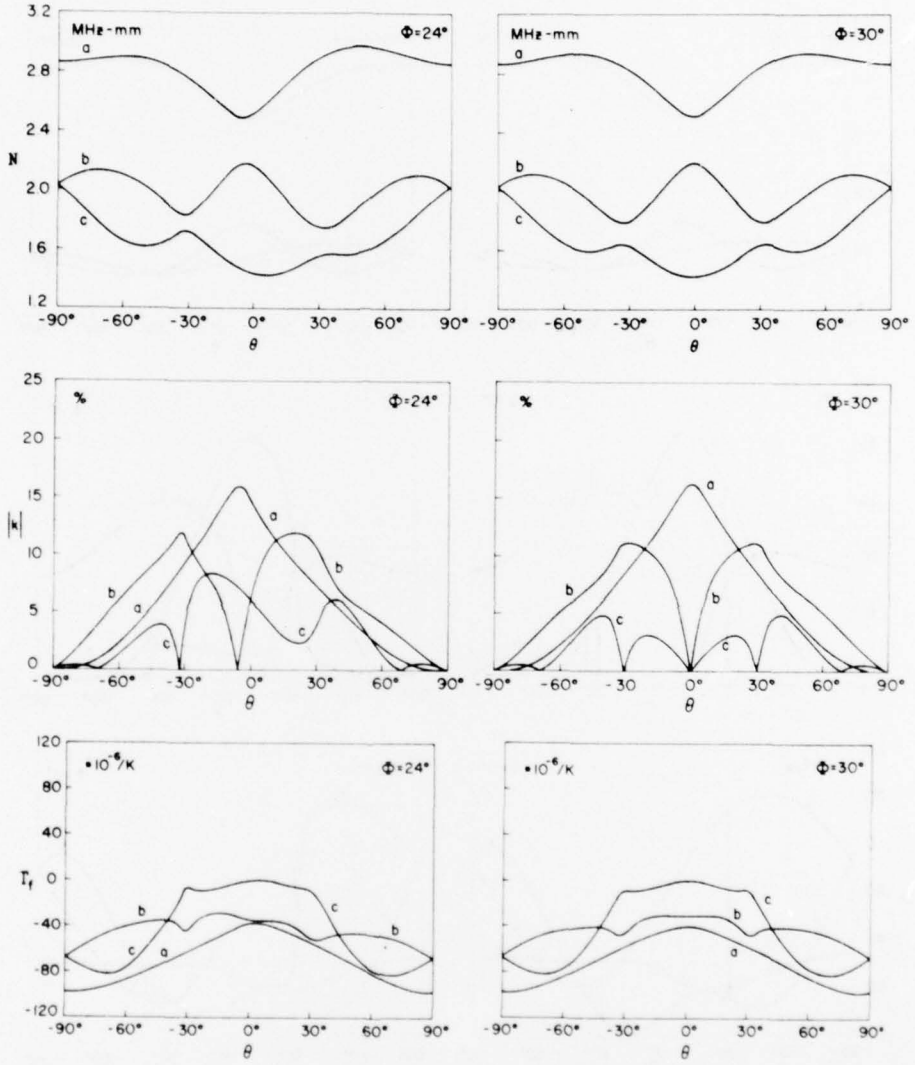


FIGURE 24. N, |k|, and $T_f$ for (YX/ωτ/θ)24°, 30°/θ Berlinite Cuts.

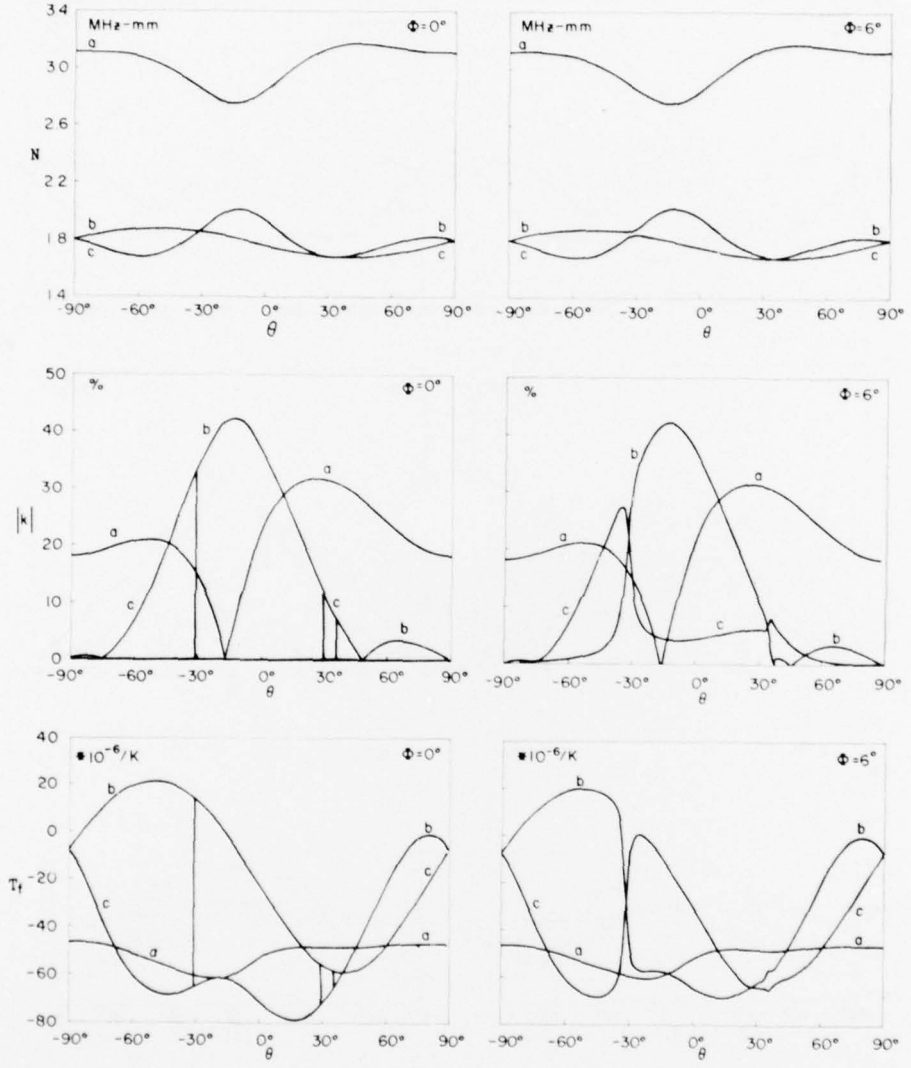


FIGURE 25. N, |k|, and $T_f$ for (YXωℓ)0°, 6°/θ $LiTaO_3$ Cuts.

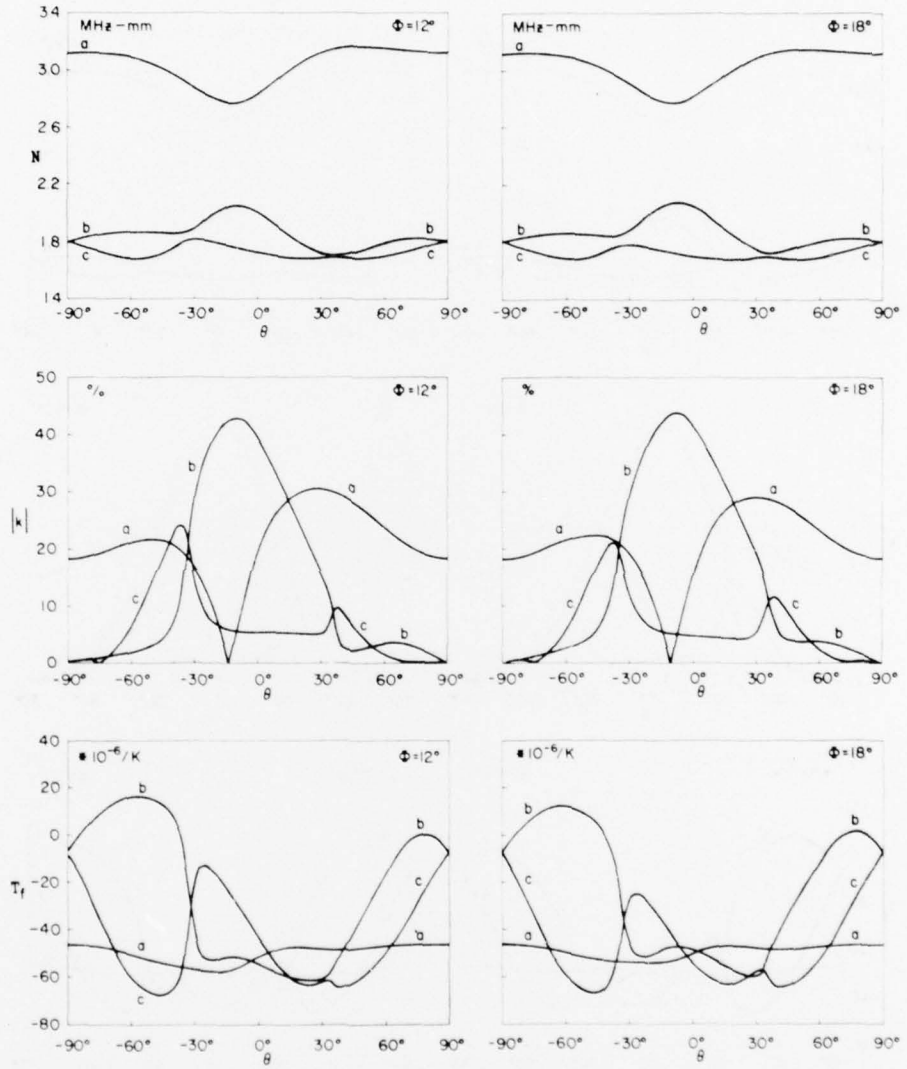


FIGURE 26. N, |k|, and $T_f$ for (YXωΦ)12°, 18°/θ $LiTaO_3$ Cuts.

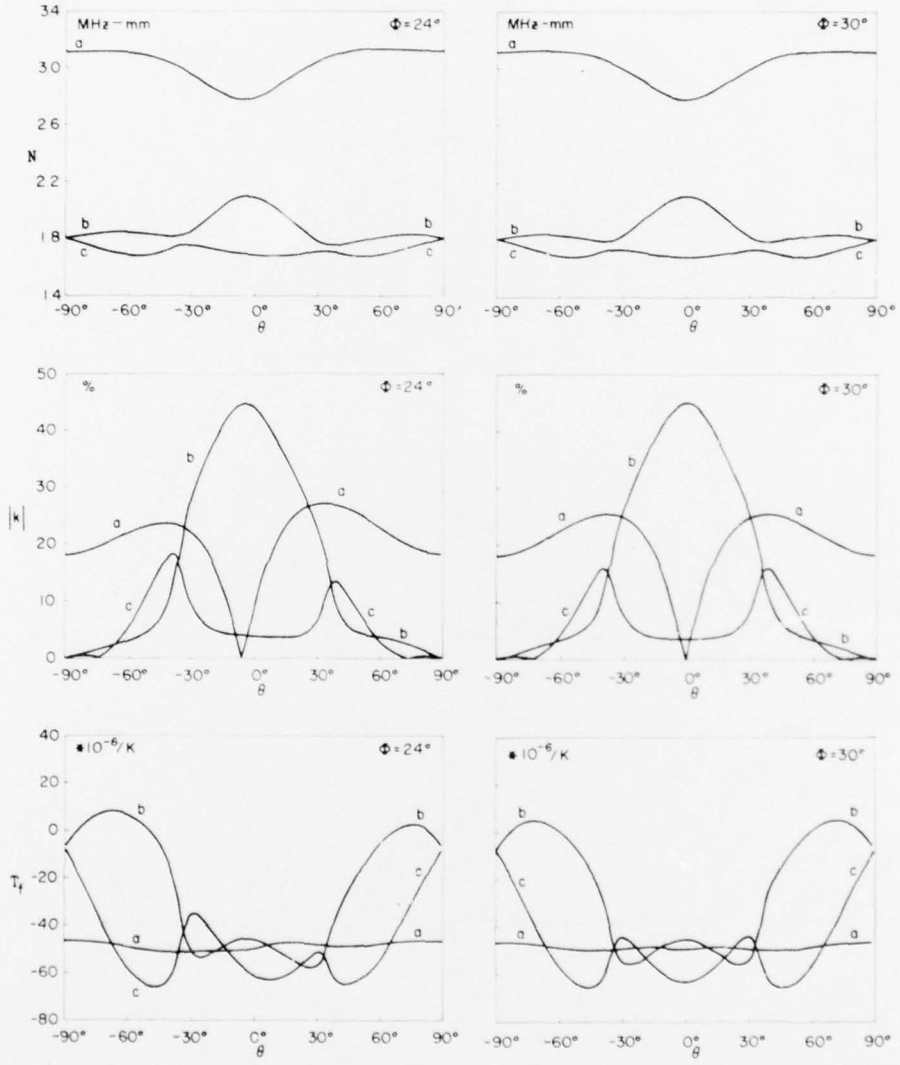


FIGURE 27. N, |k|, and $T_f$ for (YXωℓ)24°, 30°/θ $LiTaO_3$ Cuts.

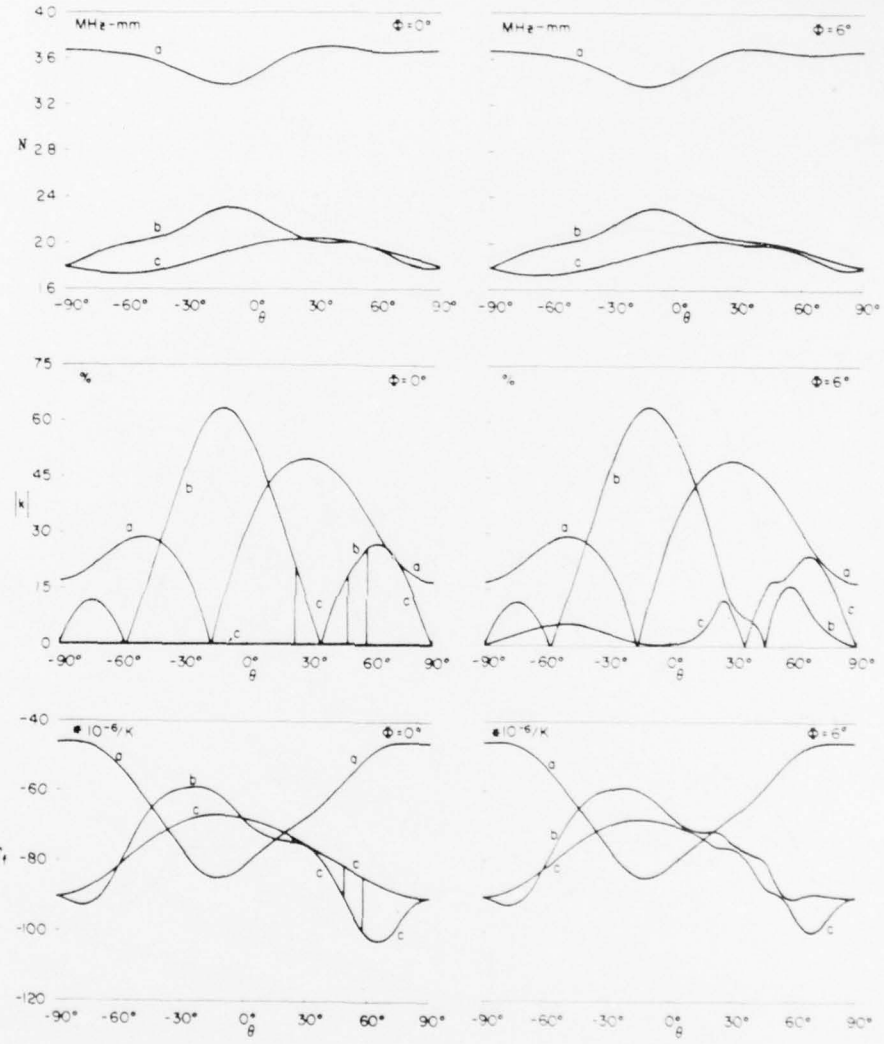


FIGURE 28. N, |k|, and $T_f$ for (YX±ω)0°, 6°/θ $LiNbO_3$ Cuts.

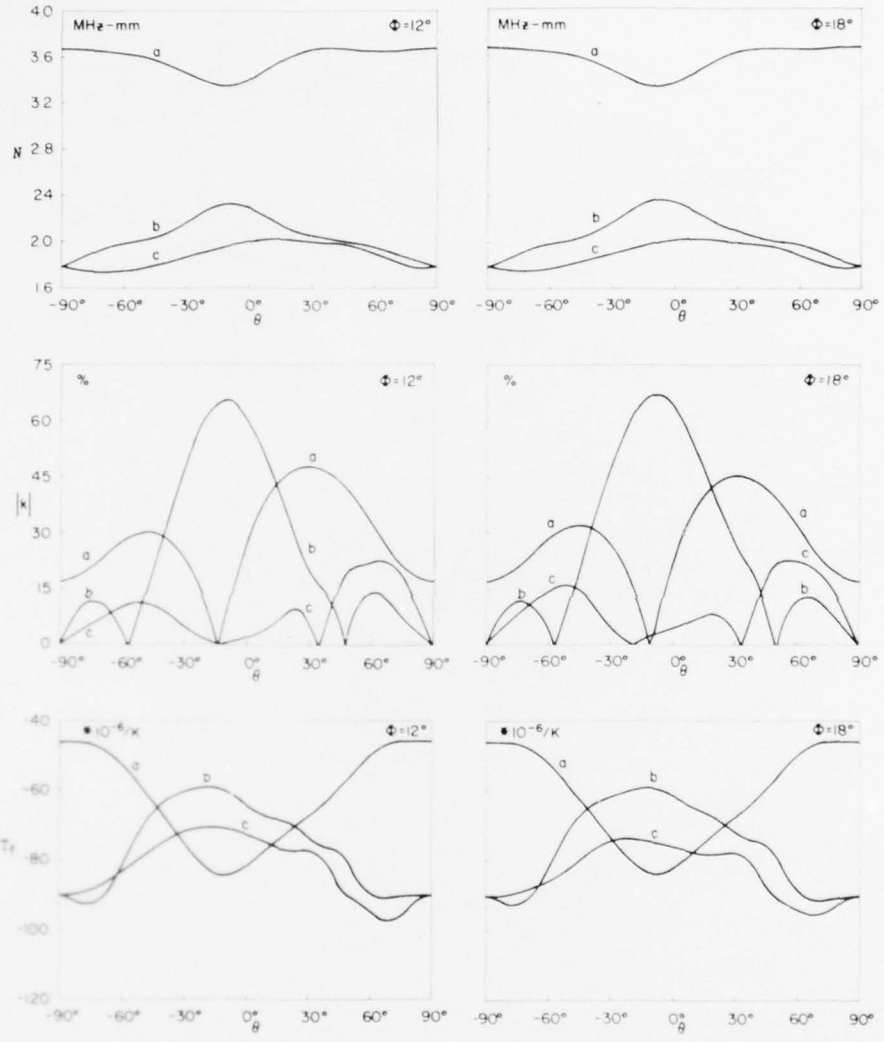


FIGURE 29. N, |k|, and $T_f$ for (YXωℓ)12°, 18°/A $LiNbO_3$ Cuts.

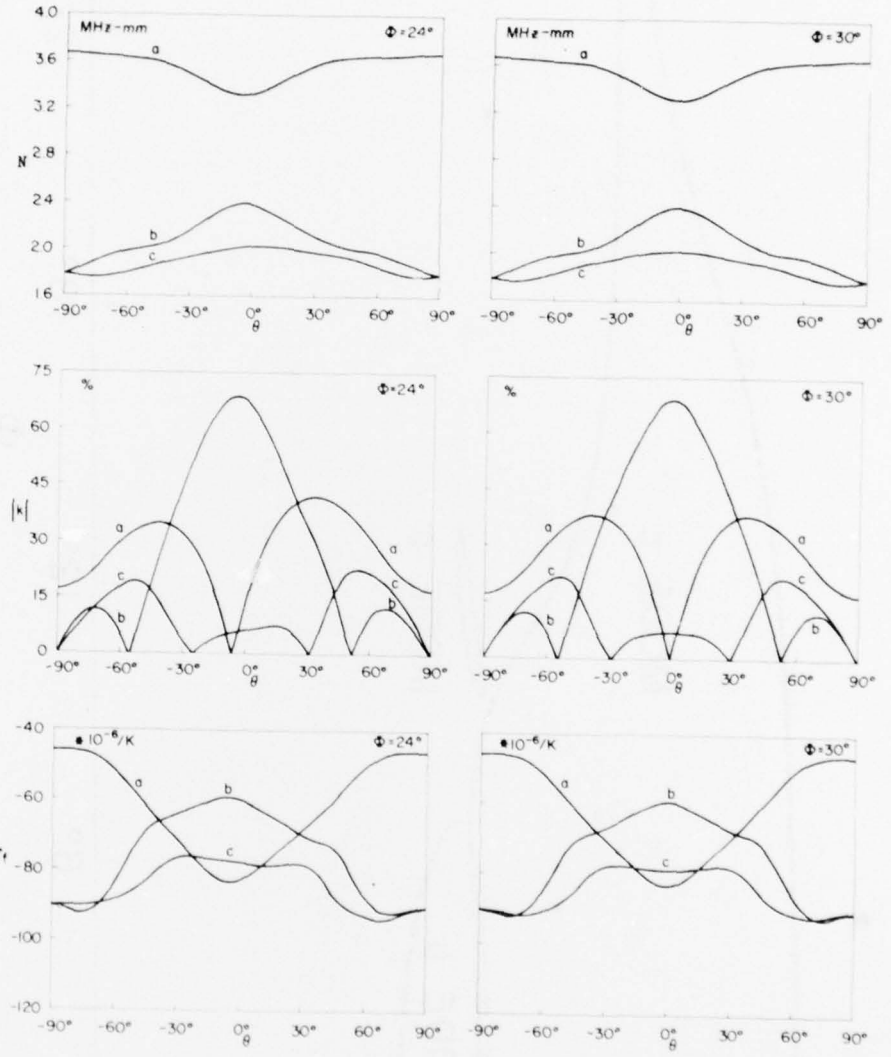


FIGURE 30. N, |k|, and $T_f$ for (YXωℓ)24°, 30°/θ $LiNbO_3$ Cuts.

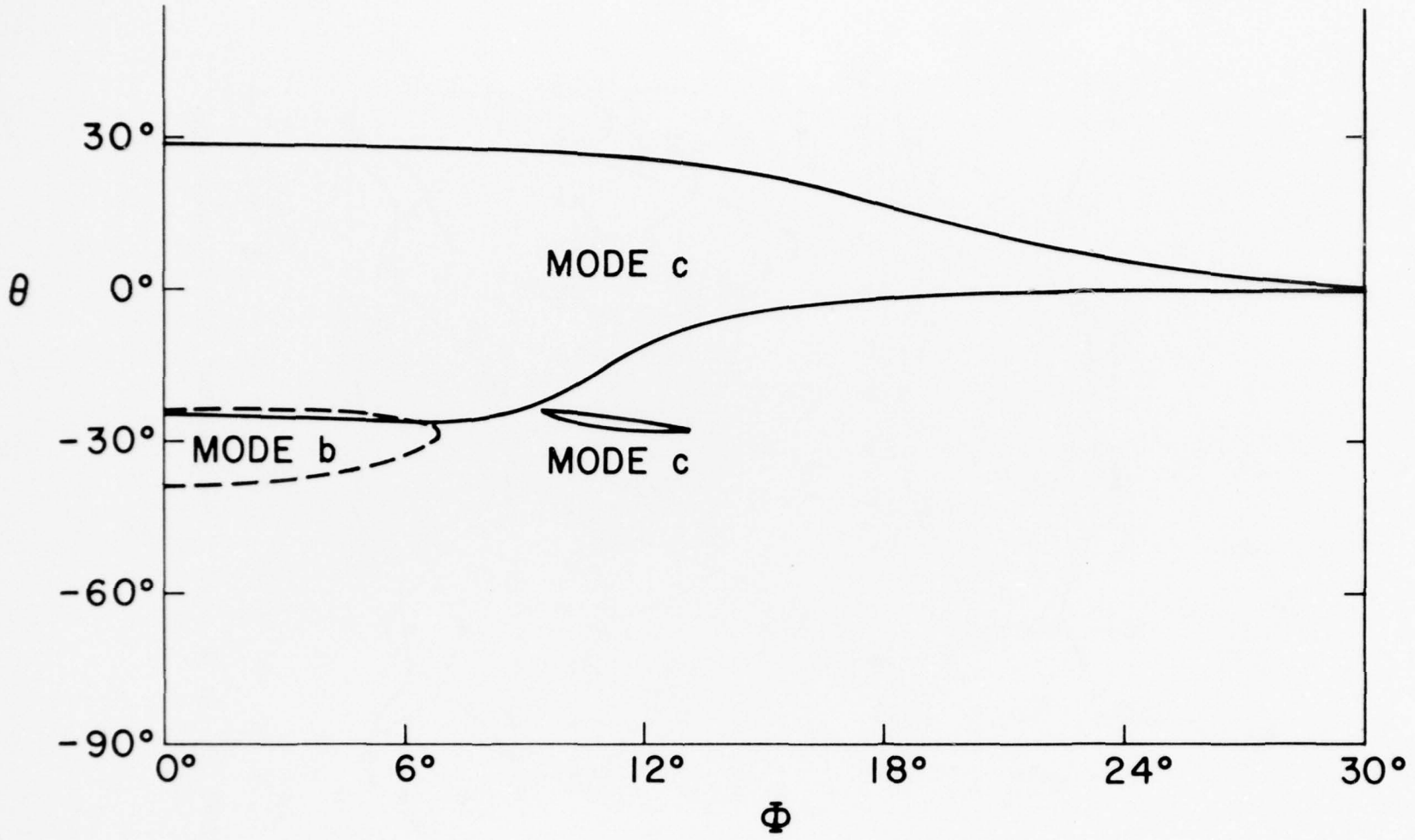


FIGURE 31. Locus of $T_f = 0$ for Doubly Rotated Cuts of Berlinite.

These BAW successes naturally lead one to hope that analogous SAW and SBAW cuts exist; if they do, it is logical to look for the SBAW cuts according to the prescription given above, viz., keeping $\emptyset$ fixed, and changing $\theta$ to $\theta+90^0$. The additional angle $\psi$, shown in Figure 10, can be adjusted for best $T\bar{C}$ or transduction efficiency.

Lewis[58] has observed non-linear interactions between SAW and SBAW in a variety of substrates.

## MATERIAL ATTENUATION

The room temperature attenuation of acoustic waves in a crystal is a function of the viscosity coefficients of the material, and has been calculated for BAW waves in quartz[41]. This intrinsic loss becomes important in the GHz range in quartz. A more severe restriction on the attenuation of GHz devices may be due to scattering losses due to etch channels[66]. These arise from chemically polishing the substrate when the source material contains impurities and dislocations; they may be largely removed by using electrically swept material.

## CONCLUSION

This report has described recent work in the area of shallow bulk acoustic waves, and has extended the applicability of bulk acoustic wave calculations to this newer type of wave propagation by giving simple rules whereby approximate results may be obtained for SBAW using BAW analyses. Both singly and doubly rotated plates have been considered, as have materials other than quartz.

REFERENCES


1. Special Issue on Microwave Acoustics, IEEE Trans. Microwave Theory Tech., Vol. MTT-17, November 1969.

2. K. Dransfeld and E. Salzmann, "Excitation, Detection, and Attenuation of High-Frequency Elastic Surface Waves", In Physical Acoustics, Principles and Methods, (W.P. Mason and R.N. Thurston, eds.), Vol. 7, Chap. 4, pp. 219-272. New York: Academic, 1970.

3. R.M. White, "Surface Elastic Waves", Proc. IEEE, Vol. 58, August 1970, pp. 1238-1276.

4. H. Sabine and P.H. Cole, "Acoustic Surface Wave Devices: A Survey", Proc. I.R.E.E. Australia, Vol. 32, December 1971, pp. 445-458.

5. R.F. Wallis, "Surface-Wave Phenomena", In Proc. Intl. School of Phys. "E. Fermi", Course LII, Atomic Structure and Properties of Solids, pp. 370-394. New York: Academic, 1972.

6. Proc. M.R.I. International Symposium XXIII, Optical and Acoustical Microelectronics, Polytechnic Institute of New York, NY 11201, Apr 1974.

7. M.G. Holland and L.T. Claiborne, "Practical Surface Acoustic Wave Devices", Proc. IEEE, Vol. 62, May 1974,pp. 582-611.

8. E. Hafner, "Crystal Resonators", IEEE Trans. Sonics Ultrason., Vol. SU-21, October 1974, pp. 220-237.

9. M.F. Lewis, "Acoustic Wave Devices", UK Patent 1,451,326, September 1976.

10. T.I. Browning and M.F. Lewis, "New Family of Bulk - Acoustic - Wave Devices Employing Interdigital Transducers", Electron. Lett., Vol. 13, March 1977, pp. 128-130; "Bulk Waves Skim the Surface", Electronics and Power, Vol. 23, February 1977, p.109.

11. T.I. Browning and M.F. Lewis, "A New Class of Quartz Crystal Oscillator Controlled by Surface-Skimming Bulk Waves", Proc. 31st Annual Frequency Control Symposium, US Army Electronics Command, Ft. Monmouth, NJ, June 1977, pp. 258-265.

12. E.G.S. Paige, "Surface Acoustic Wave Devices - A Transatlantic View", Proc. IEEE Ultrason. Symp., October 1977, pp. 563-567.

13. M.Lewis, "Surface Skimming Bulk Waves, SSBW", Proc. IEEE Ultrason. Symp. October 1977, pp. 744-752.

14. T.I. Browning, D.J. Gunton, M.F. Lewis, and C.O. Newton, "Bandpass Filters Employing Surface Skimming Bulk Waves", Proc. IEEE Ultrason. Symp. October 1977, pp. 753-756.

15. I. Browning and M. Lewis, "A New Cut of Quartz Giving Improved Stability to SAW Oscillators", Proc. 32nd Annual Frequency Control Symposium, US Army Electronics Command, Fort Monmouth, NJ, May-June 1978, pp. 87-94.

16. T.I. Browning and M.F. Lewis, "A Novel Technique for Improving the Temperature Stability of SAW/SSBW Devices", Proc. IEEE Ultrason. Symp. September 1978, pp. 474-477.

17. T.I. Browning, M.F. Lewis, and R.F. Milsom, "Surface Acoustic Waves on Rotated Y-cut $LiTaO_3$", Proc. IEEE Ultrason. Symp, September 1978, pp. 586-589.

18. H.J. Hindin and K. Smith, "Riding the Surface Acoustic Waves", Electronics, Vol. 52, No. 1, January 4, 1979, pp. 81-82.

19. K.H. Yen, K.L. Wang, and R.S. Kagiwada, "Efficient Bulk Wave Excitation on ST Quartz", Electron. Lett., Vol. 13, January 1977, pp. 37-38.

20. K.H. Yen, K.L. Wang, R.S. Kagiwada, and K.F. Lau, "Interdigital Transducers - a Means of Efficient Bulk Wave Excitation", Proc. 31st Annual Frequency Control Symposium, US Army Electronics Command, Ft. Monmouth, NJ, June 1977, pp. 266-270.

21. K.F. Lau, K.H. Yen, R.S. Kagiwada, and K.L. Wang, "Further Investigation of Shallow Bulk Acoustic Waves Generated by Using Interdigital Transducers", Proc. IEEE Ultrason. Symp., October 1977, pp. 996-1001.

22. K.H. Yen, K.F. Lau, and R.S. Kagiwada, "Temperature Stable Shallow Bulk Acoustic Wave Devices", Proc.32nd Annual Frequency Control Symposium, US Army Electronics Command, Ft. Monmouth, NJ, May-June 1978, pp.95-101.

23. K.H. Yen, K.F. Lau, and R.S. Kagiwada, "Shallow Bulk Acoustic Wave Filters", Proc. IEEE Ultrason. Symp., September 1978, pp. 680-683.

24. K.F. Lau, K.H. Yen, and R.S. Kagiwada, "Shallow Bulk Acoustic Wave Devices - A New Type of Acoustic Wave Device for Communication Systems", International Telemetering Conference, Los Angeles, CA, November 1978.

25. K.F. Lau, K.H. Yen, and R.S. Kagiwada, "Investigation of Shallow Bulk Acoustic Waves" progress report No. 1 to US Army Research Office, Research Triangle Park, NC 21709 on Contract No. DAAG29-78-C-0043, Jan 79.

26. K.H. Yen, K.F. Lau, and R.S. Kagiwada, "Energy Trapped Shallow Bulk Acoustic Waves", Electron. Lett., submitted 7 February 1979.

27. K.F. Lau, K.H. Yen, and R.S. Kagiwada, "Analysis of Shallow Bulk Acoustic Wave Excitation by Interdigital Transducers", Proc. 33rd Annual Frequency Control Symposium, US Army Electronics R&D Command, Ft. Monmouth, NJ, May-June 1979, in preparation.

28. K.H. Yen, K.F. Lau, and R.S. Kagiwada, "Narrowband and Wideband Shallow Bulk Acoustic Wave Filters", 1979 IEEE International Symposium on Circuits and Systems, Tokyo, Japan, July 1979, in preparation.

29. R.F. Mitchell, "Spurious Bulk Wave Signals in Acoustic Surface Wave Devices" Proc. IEEE Ultrason. Symp., November 1974, pp. 313-320.

30. R.S. Wagers, "Plate Modes in Surface Acoustic Wave Devices", in Physical

Acoustics: Principles and Methods", (W.P. Mason and R.N. Thurston, eds.) Vol. 13, Chap. 3. Academic Press, New York, 1977, pp. 49-78.

31. A. Jhunjhunwala, J.F. Vetelino, D. Harmon, and W. Soluch, "Theoretical Examination of Surface Skimming Bulk Waves", Proc. IEEE Ultrason. Symp., September 1978, pp. 670-674.

32. D.L. Lee, "A Theoretical Analysis of Surface Skimming Bulk Waves", Proc. IEEE Ultrason. Symp., September 1978, pp. 675-679.

33. W.S. Mortley, "Improvements in or Relating to Wave-Energy Delay Cells", UK Patent 988, 102, April 1965.

34. E.P. Papadakis, "Diffraction Grating Dispersive Delay Lines Utilizing Anisotropic Propagation Media", Ultrasonics, Vol. 8, April 1970, pp. 102-104.

35. R.M. White and F.W. Voltmer, "Direct Piezoelectric Coupling to Surface Elastic Waves", Appl. Phys. Lett., Vol. 7, December 1965, pp. 314-316.

36. "Standards on Piezoelectric Crystals, 1949", Proc. IRE, Vol. 37, December 1949, pp. 1378-1395. (IEEE Standard No. 176).

37. S.A. Bokovoy and C.F. Baldwin, "Improvements in or Relating to Piezo-Electric Crystals", UK Patent 457, 342; November 1936.

38. C.F. Baldwin and S.A. Bokovoy, "Piezoelectric Quartz Element", US Patent 2, 212, 139, August 1940.

39. C.F. Baldwin and S.A. Bokovoy, "Piezoelectric Crystal Element", US Patent 2, 254, 866, September 1941.

40. R. Bechmann, A. Ballato, and T.J. Lukaszek, "Higher-Order Temperature Coefficients of the Elastic Stiffnesses and Compliances of Alpha-Quartz", Proc. IRE, Vol. 50, August 1962, pp. 1812-1822.

41. A. Ballato, "Doubly Rotated Thickness Mode Plate Vibrators", in Physical Acoustics· Principles and Methods (W.P. Mason and R.N. Thurston, eds.) Vol. 13, Chap. 5. Academic Press, New York. 1977, pp. 115-181.

42. D.Hauden, M. Michel, and J. J. Gagnepain, "Higher Order Temperature Coefficients of Quartz SAW Oscillators", Proc. 32nd Annual Frequency Control Symposium, May-June 1978, pp. 77-86.

43. A. Ballato and T. Lukaszek, "Shallow Bulk Acoustic Wave Devices", IEEE/MTT-S International Symposium Digest, April-May 1979, pp. 162-164. IEEE Catalog No. 79CH1439-9 MTT-S.

44. A. Ballato, "Transduction of Acoustic Surface Waves by Interdigital Arrays, and Equivalent Circuit Representations", Technical Report ECOM-4359, US Army Electronics Command, Fort Monmouth, NJ 07703, October 1975, 50 pp.

45. R.F. Milsom, N.H.C. Reilly, and M. Redwood, "Analysis of Generation and

Detection of Surface and Bulk Acoustic Waves by Interdigital Transducers" IEEE Trans. Sonics Ultrason., Vol. SU-24, May 1977, pp. 147-166.

46. W.S. Mortley, "F.M.Q.", Wireless World, Vol. 57, October 1951, pp. 399-403.

47. W.S. Mortley, "Frequency-Modulated Quartz Oscillators for Broadcasting Equipment", Proc. IEE, Vol. 104B, December 1956, pp. 239-249.

48. W.S. Mortley, "Priority in Energy Trapping", Phys. Today, Vol. 19, December 1966, pp. 11-12.

49. W.H. Horton and R.C. Smythe, "The Work of Mortley and the Energy-Trapping Theory for Thickness-Shear Piezoelectric Vibrators", Proc. IEEE, Vol. 55, February 1967, p. 222.

50. W. Shockley, D.R. Curran, and D.J. Koneval, "Energy Trapping and Related Studies of Multiple Electrode Filter Crystals", Proc. 17th Annual Frequency Control Symposium, May 1963, pp. 88-126.

51. W. Shockley, D.R. Curran, and D.J. Koneval, "Trapped-Energy Modes in Quartz Filter Crystals", J. Acoust. Soc. Amer., Vol. 41, April 1967, pp. 981-993.

52. R.D. Mindlin, "Bechmann's Number for Harmonic Overtones of Thickness/Twist Vibrations of Rotated-Y-Cut Quartz Plates", J. Acoust. Soc. Amer. Vol. 41, April 1967, pp. 969-973.

53. A.A. Oliner, "Microwave Network Methods for Guided Elastic Waves", IEEE Trans. Microwave Theory Tech., Vol. MTT-17, November 1969, pp. 812-826.

54. E.A. Ash, R.M. De La Rue, and R.F. Humphryes, "Microsound Surface Waveguides", IEEE Trans. Microwave Theory Tech., Vol. MTT-17, November 1969, pp. 882-892.

55. H.F. Tiersten, "Elastic Surface Waves Guided by Thin Films", J. Appl. Phys., Vol. 40, February 1969, pp. 770-789.

56. H.F. Tiersten and R.C. Davis, "Elastic Surface Waves Guided by Curved Thin Films", J. Appl. Phys., Vol. 44, May 1973, pp. 2097-2112.

57. B.K. Sinha and H.F. Tiersten, "Elastic and Piezoelectric Surface Waves Guided by Thin Films", J. Appl. Phys., Vol. 44, November 1973, pp. 4831-4854.

58. M.F. Lewis, private communication, February 1979.

59. E.C. Jordan, Electromagnetic Waves and Radiating Systems, Englewood Cliffs, NJ: Prentice Hall, 1950, pp. 391-450.

60. E.I. Jury, Theory and Application of the z-Transform Method, New York: Wiley, 1964.

61. P.M. DeRusso, R.J. Roy, and C.M. Close, State Variables for Engineers,

New York: Wiley, 1965, pp. 158-186.

62. H. Gautier and G.S. Kino, "A Detailed Theory of the Acoustic Wave Semiconductor Convolver", IEEE Trans. Sonics Ultrason., Vol. SU-24, January 1977, pp. 23-33.

63. B.T. Khuri-Yakob and G.S. Kino, "A Detailed Theory of the Monolithic Zinc Oxide on Silicon Convolver", IEEE Trans. on Sonics Ultrason., Vol. SU-24, January 1977, pp. 34-43.

64. E.P. EerNisse, T. Lukaszek, and A. Ballato, "Variational Calculation of Force-Frequency Constants of Doubly Rotated Quartz Resonators", IEEE Trans. Sonics Ultrason., Vol. SU-25, May 1978, pp. 132-138.

65. A. Ballato, "Static and Dynamic Behavior of Quartz Resonators", IEEE Trans. Sonics Ultrason., Vol. SU-26, July 1979, in press.

66. J.R. Vig, J.W. LeBus and R.L. Filler, "Chemically Polished Quartz", Proc. 31st Annual Frequency Control Symposium, June 1977, US Army Electronics Command, Fort Monmouth, NJ 07703, pp. 131-143